

Valence bond solids for $SU(n)$ spin chains: exact models, spinon condensation, and the Haldane gap

Martin Greiter and Stephan Rachel
Institut für Theorie der Kondensierten Materie,
Universität Karlsruhe, Postfach 6980,
76128 Karlsruhe, Germany

To begin with, we introduce several exact models for $SU(3)$ spin chains: (1) a translationally invariant parent Hamiltonian involving four-site interactions for the trimer chain, with a three-fold degenerate ground state. We provide numerical evidence that the elementary excitations of this model transform under representation 3 of $SU(3)$ if the original spins of the model transform under rep. 3. (2) a family of parent Hamiltonians for valence bond solids of $SU(3)$ chains with spin reps. 6, 10, and 8 on each lattice site. We argue that of these three models, only the latter two exhibit spinon condensation and hence a Haldane gap in the excitation spectrum. We generalize some of our models to $SU(n)$. Finally, we use the emerging rules for the construction of VBS states to argue that models of antiferromagnetic chains of $SU(n)$ spins in general possess a Haldane gap if the spins transform under a representation corresponding to a Young tableau consisting of a number of boxes which is divisible by n . If n and n have no common divisor, the spin chain will support deconfined spinons and not exhibit a Haldane gap. If n and n have a common divisor different from n , it will depend on the specifics of the model including the range of the interaction.

PACS numbers: 75.10.Jm, 75.10.Pq, 75.10.Dg, 32.80.Pj

I. INTRODUCTION

Quantum spin chains have been a most rewarding subject of study almost since the early days of quantum mechanics, beginning with the invention of the Bethe ansatz in 1931 [1] as a method to solve the $S = \frac{1}{2}$ Heisenberg chain with nearest-neighbor interactions. The method led to the discovery of the Yang-Baxter equation in 1967 [2, 3], and provides the foundation for the field of integrable models [4]. Faddeev and Takhtajan [5] discovered in 1981 that the elementary excitations (now called spinons) of the spin-1=2 Heisenberg chain carry spin 1=2 while the Hilbert space is spanned by spin 1's, which carry spin 1. The fractional quantization of spin in spin chains is conceptually similar to the fractional quantization of charge in quantized Hall liquids [6, 7]. In 1982, Haldane [8, 9] identified the $O(3)$ nonlinear sigma model as the effective low-energy field theory of $SU(2)$ spin chains, and argued that chains with integer spin possess a gap in the excitation spectrum, while a topological term renders half-integer spin chains gapless [10, 11].

The general methods [the Bethe ansatz method and the use of effective field theories including bosonization [12, 13]] are complemented by a number of exactly solvable models, most prominently among them the Majumdar-Ghosh (MG) Hamiltonian for the $S = \frac{1}{2}$ dimer chain [14], the AKLT model as a paradigm of the gapped $S = 1$ chain [15, 16], and the Haldane-Shastry model (HSM) [17, 20]. The HSM is by far the most sophisticated among these three, as it is not only solvable for the ground state, but fully integrable due to its Yangian symmetry [20]. The wave functions for the ground state and single-spinon excitations are of a simple Jastrow form, elevating the conceptual similarity to quantized Hall states to a formal equivalence. Another unique

feature of the HSM is that the spinons are free in the sense that they only interact through their half-Fermi statistics [21-25], which renders the model an ideal starting point for any perturbative description of spin systems in terms of interacting spinons [26]. The HSM has been generalized from $SU(2)$ to $SU(n)$ [27-32].

For the MG and the AKLT model, only the ground states are known exactly. Nonetheless, these models have amply contributed to our understanding of many aspects of spin chains, each of them through the specific concepts captured in its ground state [33-51]. The models are specific to $SU(2)$ spin chains. We will review both models below.

In the past, the motivation to study $SU(n)$ spin systems with $n > 2$ has been mainly formal. The Bethe ansatz method has been generalized to multiple component systems by Sutherland [52], yielding the so-called nested Bethe ansatz. In particular, this has led to a deeper understanding of quantum integrability and the applicability of the Bethe ansatz [53]. Furthermore, the nested Bethe ansatz was used to study the spectrum of the $SU(n)$ HSM [22, 27]. It has also been applied to $SU(2)$ spin chains with orbital degeneracy at the $SU(4)$ symmetric point [54, 55]. Most recently, Damara and Klumper obtained highly accurate numerical results for the thermodynamic properties of the $SU(4)$ spin-orbital model [56]. $SU(n)$ Heisenberg models have been studied recently by Kawashima and Tanabe [57] with quantum Monte Carlo, and by Paramakanti and Marston [58] using variational wave functions.

The effective field theory description of $SU(2)$ spin chains by Haldane yielding the distinction between gapless half-integer spin chains with deconfined spinons and gapped integer spin chains with confined spinons cannot be directly generalized to $SU(n)$, as there is no direct

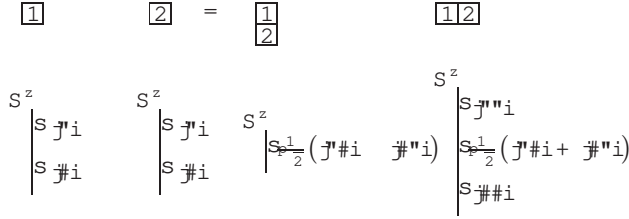


FIG. 1: Tensor product of two $S = \frac{1}{2}$ spins with Young tableaux and weight diagrams of the occurring $SU(2)$ representations. S^z is the diagonal generator.

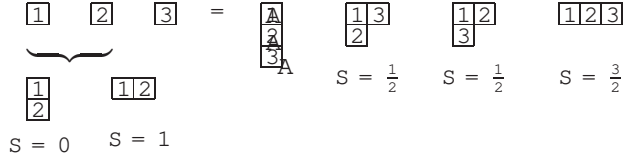


FIG. 2: Tensor product of three $S = \frac{1}{2}$ spins with Young tableaux. For $SU(n)$ with $n > 2$, the tableau with three boxes on top of each other exists as well.

using the operator P_{ij} , which permutes the $SU(n)$ spins (here $n = 3$) on sites i and j :

$$J_i J_j = \frac{1}{2} P_{ij} - \frac{1}{n} : \quad (13)$$

To verify the trimer Hamiltonian (12), as well as for the valence bond solid (VBS) models we propose below, we will need a few higher-dimensional representations of $SU(3)$. We review these in the following section.

IV. REPRESENTATIONS OF $SU(3)$

A. Young tableaux and representations of $SU(2)$

Let us begin with a review of Young tableaux and the representations of $SU(2)$. The group $SU(2)$ has three generators S^a , $a = 1, 2, 3$, which obey the algebra

$$S^a S^b = i \epsilon^{abc} S^c; \quad (14)$$

where repeated indices are summed over and ϵ^{abc} is the totally antisymmetric tensor. The representations of $SU(2)$ are classified by the spin S , which takes integer or half-integer values. The fundamental representation of $SU(2)$ has spin $S = \frac{1}{2}$, it contains the two states $|\uparrow\rangle$ and $|\downarrow\rangle$. Higher-dimensional representations can be constructed as tensor products of fundamental representations, which is conveniently accomplished using Young tableaux (see e.g. [66]). These tableaux are constructed as follows (see Figs. 1 and 2 for examples). For each of the N spins, draw a box numbered consecutively from left to right. The representations of $SU(2)$ are obtained by putting the boxes together such that the numbers assigned to them increase in each row from left to right and

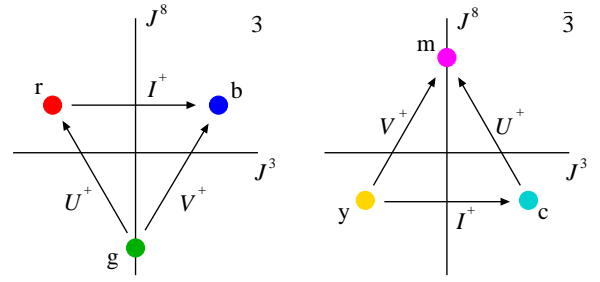


FIG. 3: (Color online) a) Weight diagram of the fundamental $SU(3)$ representation $3 = (1;0)$. b) Weight diagram of the complex conjugate representation $\bar{3} = (0;1)$. J^3 and J^8 denote the diagonal generators, U^+ , U^- , and V^+ , V^- the raising and lowering operators.

in each column n from top to bottom. Each tableau indicates symmetrization over all boxes in the same row, and antisymmetrization over all boxes in the same column. This implies that we cannot have more than two boxes on top of each other. If i denotes the number of boxes in the i th row, the spin is given by $S = \frac{1}{2} (i_1 - i_2)$.

To be more explicit, let us consider the tensor product $\frac{1}{2} \otimes \frac{1}{2} \otimes \frac{1}{2}$ depicted in Fig. 2 in detail. We start with the state $\frac{3}{2}; \frac{3}{2} = |\uparrow\uparrow\uparrow\rangle$, and hence find

$$\frac{3}{2}; \frac{3}{2} = \frac{1}{\sqrt{3}} S^+ |\uparrow\uparrow\uparrow\rangle = \frac{1}{\sqrt{3}} (|\uparrow\uparrow\downarrow\rangle + |\uparrow\downarrow\uparrow\rangle + |\downarrow\uparrow\uparrow\rangle); \quad (15)$$

The two states with $S = S^z = \frac{1}{2}$ must be orthogonal to (15). A convenient choice of basis is

$$\begin{aligned} \frac{1}{2}; \frac{1}{2}; + &= \frac{1}{\sqrt{3}} (|\uparrow\uparrow\downarrow\rangle + |\uparrow\downarrow\uparrow\rangle + |\downarrow\uparrow\uparrow\rangle); \\ \frac{1}{2}; \frac{1}{2}; - &= \frac{1}{\sqrt{3}} (|\uparrow\uparrow\downarrow\rangle - |\uparrow\downarrow\uparrow\rangle - |\downarrow\uparrow\uparrow\rangle); \end{aligned} \quad (16)$$

where $! = \exp i \frac{2\pi}{3}$. The tableaux tell us primarily that two such basis states exist, not what a convenient choice of orthonormal basis states may be.

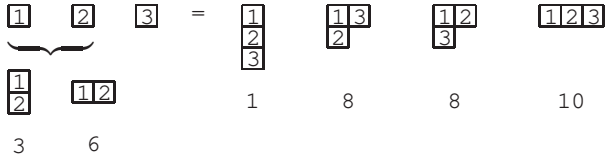
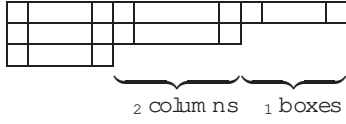
The irreducible representations of $SU(2)$ can be classified through the eigenvalues of the Casimir operator given by the square of the total spin S^2 . The special feature of S^2 is that it commutes with all generators S^a and is hence by Schur's lemma [67] proportional to the identity for any finite-dimensional irreducible representation. The eigenvalues are given by

$$S^2 = C_{SU(2)}^2 = S(S+1);$$

B. Representation theory of $SU(3)$

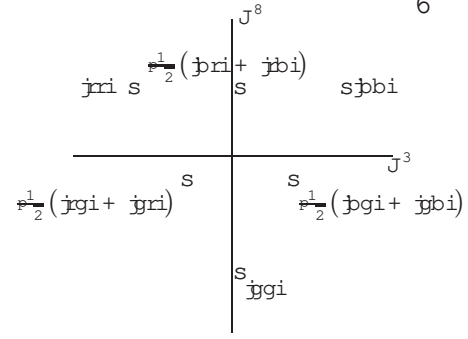
The group $SU(3)$ has eight generators J^a , $a = 1, \dots, 8$, which obey the algebra

$$J^a J^b = f^{abc} J^c; \quad (17)$$

FIG. 4: Tensor product $3 \times 3 \times 3$ with Young tableaux.FIG. 5: Dynkin coordinates $(\lambda_1; \lambda_2)$ for a given Young tableau. The columns containing three boxes represent additional SU(3) singlet factors, which yield equivalent representations and hence leave the Dynkin coordinates $(\lambda_1; \lambda_2)$ unchanged.

where the structure constants f^{abc} are given in App. B. For SU(3) we have two diagonal generators, usually chosen to be J^3 and J^8 , and six generators which define the ladder operators $I = J^1 - iJ^2$, $U = J^6 - iJ^7$, and $V = J^4 - iJ^5$, respectively. An explicit realization of (17) is, for example, given by the J^a 's as expressed in terms of Gell-Mann matrices in (9). This realization defines the fundamental representation 3 of SU(3) illustrated in Fig. 3a. It is three-dimensional, and we have chosen to label the basis states by the colors blue (b), red (r), and green (g). The weight diagram depicted in Fig. 3a instructs us about the eigenvalues of the diagonal generators as well as the actions of the ladder operators on the basis states.

All other representations of SU(3) can be constructed by taking tensor products of reps. 3, which is again most conveniently accomplished using Young tableaux (see Fig. 4 for an example). The antisymmetrization over all boxes in the same column implies that we cannot have more than three boxes on top of each other. Each tableau stands for an irreducible representation of SU(3), which can be uniquely labeled by their highest weight or Dynkin coordinates $(\lambda_1; \lambda_2)$ [67, 68] (see Fig. 5). For example, the fundamental representation 3 has Dynkin coordinates (1,0). Note that all columns containing three boxes are superfluous, as the antisymmetrization of three colors yields only one state. In particular, the SU(3) singlet has Dynkin coordinates (0,0). In general, the dimension of a representation $(\lambda_1; \lambda_2)$ is given by $\frac{1}{2}(\lambda_1 + 1)(\lambda_2 + 1)(\lambda_1 + \lambda_2 + 2)$. The labeling using bold numbers refers to the dimensions of the representations alone. Although this labeling is not unique, it will mostly be sufficient for our purposes. A representation m and its conjugated counterpart \bar{m} are related to each other by interchange of their Dynkin coordinates.

FIG. 6: Weight diagram of the representation $6 = (2;0)$. The weight diagram of the conjugate representation $\bar{6} = (0;2)$ is obtained by reflection at the origin [67].

C. Examples of representations of SU(3)

We now consider some specific representations of SU(3) in detail. As a starting point we use the fundamental representation 3 spanned by the states jbi , jri , and jgi . The second three-dimensional representation $\bar{3}$ is obtained by antisymmetrically coupling two reps. 3. The Dynkin coordinates of the rep. $\bar{3}$ are (0,1), i.e., the reps. 3 and $\bar{3}$ are complex conjugate of each other. An explicit basis of the rep. $\bar{3}$ is given by the colors yellow (y), cyan (c), and magenta (m),

$$\begin{aligned} jyi &= \frac{1}{\sqrt{2}} jgi - jri; \\ jci &= \frac{1}{\sqrt{2}} jbi - jgi; \\ jmi &= \frac{1}{\sqrt{2}} jri - jbi. \end{aligned} \quad (18)$$

The weight diagram is shown in Fig. 3b. The generators are given by (9) with a replaced by (\bar{a}) , where \bar{a} denotes complex conjugation of the matrix elements [68]. In particular, we find $I^+ jyi = jci$, $U^+ jci = jmi$, and $V^+ jmi = jbi$.

The six-dimensional representation 6 has Dynkin coordinates (2,0), and can hence be constructed by symmetrically coupling two reps. 3. The basis states of the rep. 6 are shown in Fig. 6. The conjugate representation $\bar{6}$ can be constructed by symmetrically coupling two reps. $\bar{3}$.

Let us now consider the tensor product $3 \times 3 = 1 + 8$. The weight diagram of the so-called adjoint representation $8 = (1;1)$ is shown in Fig. 7. The states can be constructed starting from the highest weight state jmi , yielding $I jmi = jmi$, $U jmi = jci$, $V jmi = jgi$, and so on. This procedure yields two linearly independent states with $J^3 = J^8 = 0$. The representation 8 can also be obtained by coupling of the reps. 6 and $\bar{3}$, as can be seen from the Young tableaux in Fig. 4. On a more abstract level, the adjoint representation is the representation we obtain if we consider the generators J^a themselves as basis vectors. In the weight diagram

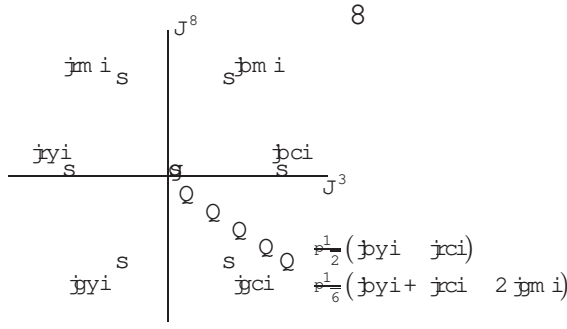


FIG. 7: Weight diagram of the adjoint representation $8 = (1;1)$. The state with $J^3 = J^8 = 0$ is doubly degenerate [67]. Note that two reps. 8 can be constructed by combining three fundamental reps. 3 (colors), just as two reps. $\frac{1}{2}$ can be constructed by combining three SU(2) spins (cf. (16)). The states in the diagram span a basis for one of these representations.

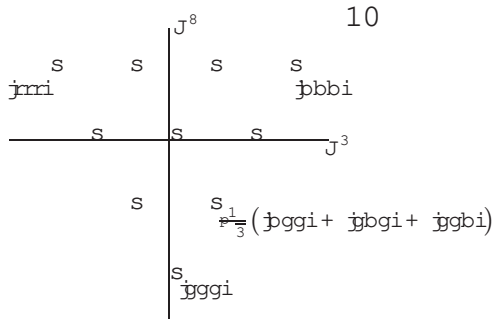


FIG. 8: Weight diagram of the representation $10 = (3;0)$. The weight diagram of the conjugate representation $\bar{10} = (0;3)$ is obtained by reflection at the origin [67].

shown in Fig. 7, the generators J^3 and J^8 correspond to the two states at the origin, whereas the ladder operators I , U , and V correspond to the states at the six surrounding points. In the notation of Fig. 7, the singlet orthogonal to 8 is given by $\frac{1}{3}(jyi + jci + jmi)$.

The weight diagrams of four other representations relevant to our purposes below are shown in Figs. 8 to 10.

It is known that the physical properties of SU(2) spin chains crucially depend on whether on the lattice sites are integer or half-integer spins. A similar distinction can be made for SU(3) chains, as elaborated in Sec. X. The distinction integer or half-integer spin for SU(2) is replaced by a distinction between three families of irreducible representations of SU(3): either the number of boxes in the Young tableau is divisible by three without remainder (e.g. 1, 8, 10, 27), with remainder one (e.g. 3, 6, 15, 15^0), or with remainder two (e.g. 3, 6, $\bar{15}$, $\bar{15}^0$).

While SU(2) has only one Casimir operator, SU(3) has two. The quadratic Casimir operator is defined as

$$J^2 = \sum_{a=1}^8 J^a J^a; \quad (19)$$

where the J^a 's are the generators of the representation.

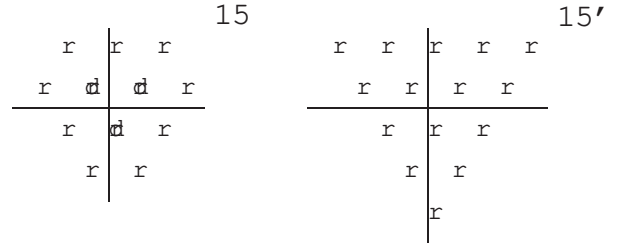


FIG. 9: Weight diagram of the representations $15 = (2;1)$ and $15^0 = (4;0)$.

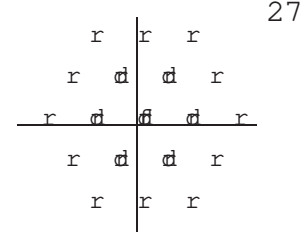


FIG. 10: Weight diagram of the self-conjugate representation $27 = (2;2)$. The state with $J^3 = J^8 = 0$ is three-fold degenerate [67].

As J^2 commutes with all generators J^a it is proportional to the identity for any finite-dimensional irreducible representation. The eigenvalue in a representation with Dynkin coordinates $(\lambda_1; \lambda_2)$ is [67]

$$J^2 = C_{\text{SU}(3)}^2(\lambda_1; \lambda_2) = \frac{1}{3}(\lambda_1^2 + \lambda_1\lambda_2 + \lambda_2^2 + 3\lambda_1 + 3\lambda_2); \quad (20)$$

We have chosen the normalization in (19) according to the convention

$$C_{\text{SU}(n)}^2(\text{adjoint representation}) = n;$$

which yields $C_{\text{SU}(3)}^2(1;1) = 3$ for the representation 8. Note that the quadratic Casimir operator cannot be used to distinguish between a representation and its conjugate. This distinction would require the cubic Casimir operator [67], which we will not need for any of the models we propose below.

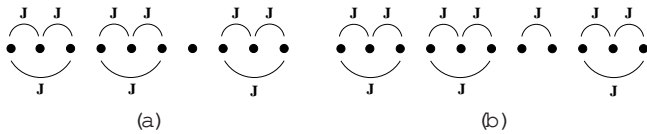
V. THE TRIMER MODEL (CONTINUED)

B. Verification of the model

We will now proceed with the verification of the trimer Hamiltonian (12). Since the spins on the individual sites transform under the fundamental representation 3, the SU(3) content of four sites is

$$3 \otimes 3 \otimes 3 \otimes 3 = 3 \oplus 3 \oplus 26 \oplus 3 \oplus 15 \oplus \bar{15}; \quad (21)$$

i.e., we obtain representations 3, 6, and two non-equivalent 15-dimensional representations with Dynkin



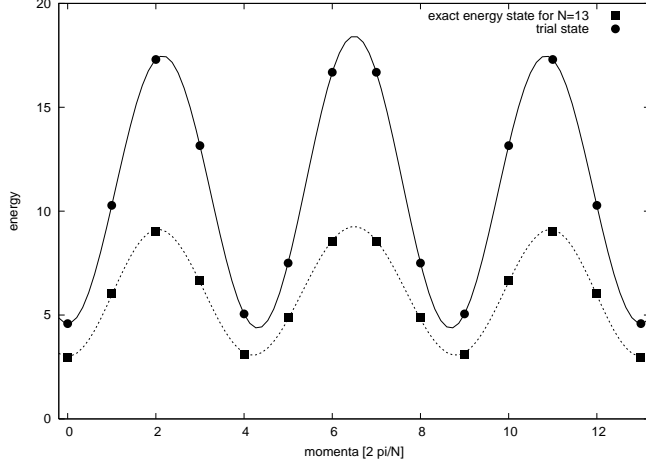


FIG. 12: Dispersion of the rep. 3 trial states (23) in comparison to the exact excitation energies of (12) for a chain with $N = 13$. The lines are a guide to the eye.

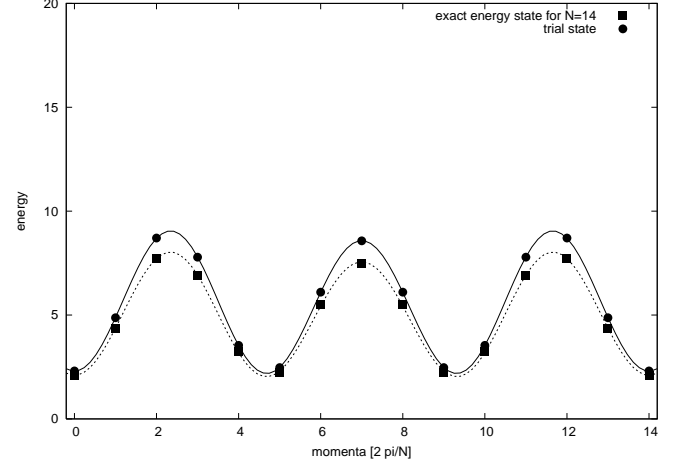


FIG. 13: Dispersion of the rep. 3 trial states (24) in comparison to the exact excitation energies of (12) for a chain with $N = 14$. The lines are a guide to the eye.

mom [$2\pi/N$]	E_{tot}		%	over-
	exact	trial	o	lap
0	2.1013	2.3077	9.8	0.9953
1, 13	4.3677	4.8683	11.5	0.9864
2, 12	7.7322	8.7072	12.6	0.9716
3, 11	6.8964	7.7858	12.9	0.9696
4, 10	3.2244	3.5415	9.8	0.9934
5, 9	2.2494	2.4690	9.7	0.9950
6, 8	5.4903	6.1016	11.1	0.9827
7	7.4965	8.5714	14.3	0.9562

TABLE II: Energies of the rep. 3 trial states (24) in comparison to the exact excitation energies of the trimer model (12) and their overlaps for an $SU(3)$ spin chain with $N = 14$ sites.

The numerical results clearly indicate that the rep. 3 trial states (24) are valid approximations to the elementary excitations of the trimer chain, while the rep. 3 trial states (23) are not. We deduce that the elementary excitations of the trimer chain (12) transform under 3, that is, under the representation conjugated to the original $SU(3)$ spins localized at the sites of the chain. Using the language of colors, one may say that if a basis for the original spins is spanned by blue, red, and green, a basis for the excitations is spanned by the complementary colors yellow, cyan, and magenta. This result appears to be a general feature of $SU(3)$ spin chains, as it was recently shown explicitly to hold for the Haldane-Shastry model as well [30, 32].

Note that the elementary excitations of the trimer chain are deconfined, meaning that the energy of two localized representation 3 domain walls or colorons (24) does not depend on the distance between them. The

reason is simply that domain walls connect one ground state with another, without introducing costly correlations in the region between the domain walls. In the case of the MG model and the trimer model introduced here, however, there is still an energy gap associated with the creation of each coloron, which is simply the energy cost associated with the domain wall.

In most of the remainder of this article, we will introduce a family of exactly soluble valence bond models for $SU(3)$ chains of various spin representations of the $SU(3)$ spins at each lattice site. To formulate these models, we will first review Schwinger bosons for both $SU(2)$ and $SU(3)$ and the AKLT model.

V I. SCHWINGER BOSONS

Schwinger bosons [69, 70] constitute a way to formulate spin- S representations of an $SU(2)$ algebra. The spin operators

$$\begin{aligned} S^x + iS^y &= S^+ = a^\dagger b; \\ S^x - iS^y &= S^- = b^\dagger a; \\ S^z &= \frac{1}{2}(a^\dagger a - b^\dagger b); \end{aligned} \quad (25)$$

are given in terms of boson creation and annihilation operators which obey the usual commutation relations

$$\begin{aligned} a^\dagger a^\dagger &= b^\dagger b^\dagger = 0; \\ a^\dagger b &= a b^\dagger = a^\dagger b^\dagger = a b = 0; \end{aligned} \quad (26)$$

It is readily verified with (26) that S^x , S^y , and S^z satisfy (14). The spin quantum number S is given by half the number of bosons,

$$2S = a^\dagger a + b^\dagger b; \quad (27)$$

is the exact zero-energy ground state of the spin-1 extended Heisenberg Hamiltonian

$$H_{AKLT} = \sum_i S_i S_{i+1} + \frac{1}{3} S_i S_{i+1}^2 + \frac{2}{3} \quad (40)$$

with periodic boundary conditions. Each term in the sum (40) projects onto the subspace in which the total spin of a pair of neighboring sites is $S = 2$. The Hamiltonian (40) thereby lifts all states except (39) to positive energies. The VBS state (39) is a generic paradigm as it shares all the symmetries, but in particular the Haldane spin gap [8, 9, 34], of the spin-1 Heisenberg chain. It even offers a particularly simple understanding of this gap, or of the linear confinement potential between spinons responsible for it, as illustrated by the cartoon:

Our understanding [71, 72] of the connection between the confinement force and the Haldane gap is that the confinement effectively imposes an oscillator potential for the relative motion of the spinons. We then interpret the zero-point energy of this oscillator as the Haldane gap in the excitation spectrum.

The AKLT state can also be written as a matrix product [42, 44, 45]. We first rewrite the valence bonds

$$a_i^y b_{i+1}^y \quad b_i^y a_{i+1}^y = a_i^y b_i^y \quad b_{i+1}^y a_{i+1}^y ; \quad !$$

and then use the outer product to combine the two vectors at each site into a matrix

$$M_i = \begin{pmatrix} b_i^y & a_i^y b_i^y \\ a_i^y & b_i^y \end{pmatrix} \quad j0 i_i \quad ! \quad (41)$$

$$= \begin{pmatrix} j1; 0 i_i & p \overline{2} j1; 1 i_i \\ p \overline{2} j1; 1 i_i & j1; 0 i_i \end{pmatrix} :$$

Assuming PBCs, (39) may then be written as the trace of the matrix product

$$j_{AKLT} i = \text{tr} \sum_i M_i : \quad (42)$$

In the following section, we will propose several exact models of VBSs for $SU(3)$.

VIII. $SU(3)$ VALENCE BOND SOLIDS

To begin with, we use $SU(3)$ Schwinger bosons introduced in Sec. VI to rewrite the trimer states (7) as

$$\begin{pmatrix} E \\ \text{trimer} \end{pmatrix} = \sum_{(i; \text{integer})}^Y \sum_{(b; r; g)}^X \text{sign} \begin{pmatrix} Y \\ i \quad i+1 \quad i+2 \end{pmatrix} j0 i \quad b^y; r^y; g^y \quad j0 i; \quad (43)$$

where, as in (7), $i = 1; 2; 3$ labels the three degenerate ground states, i runs over the lattice sites subject to the constraint that $\frac{i}{3}$ is integer, and the sum extends over all six permutations of the three colors b , r , and g . This formulation can be used directly to construct VBSs for $SU(3)$ spin chains with spins transforming under representations 6 and 10 on each site.

A. The representation 6 VBS

We obtain a representations 6 VBS from two trimer states by projecting the tensor product of two fundamental representations 3 onto the symmetric subspace, i.e., onto the 6 in the decomposition $3 \otimes 3 = 3 \oplus 6$. Graphically, this is illustrated as follows:

This construction yields three linearly independent 6 VBS states, as there are three ways to choose two different trimer states out of a total of three. These three VBS states are readily written out using (43),

$$\begin{pmatrix} E \\ 6_{VBS} \end{pmatrix} = \begin{pmatrix} b^y; r^y; g^y \\ +1 \quad b^y; r^y; g^y \end{pmatrix} j0 i \quad (45)$$

for $i = 1, 2$, or 3. If we pick four neighboring sites on a chain with any of these states, the total $SU(3)$ spin of those may contain the representations

$$\begin{pmatrix} 3 & 3 \\ 3 & 3 \end{pmatrix} \triangleq 3 \otimes 3 = 3 \oplus 6$$

or the representations

$$\begin{pmatrix} 3 & 3 \\ 3 & 3 \end{pmatrix} \triangleq 3 \otimes 3 = 2 \oplus 3 \oplus 6 \oplus \overline{15};$$

i.e., the total spin transforms under 3, 6, or $\overline{15} = (1; 2)$, all of which are contained in the product

$$\begin{matrix} 6 & 6 & 6 & 6 \\ 3 & \overline{3} & 6 & 6 \end{matrix} \begin{matrix} \overline{7} & 15 & \overline{3}^0 & 153 \\ 8 & 24 & 6 & 42 \end{matrix} \begin{matrix} 45 & 6 & 60 & 3 \end{matrix} \begin{matrix} 63 \\ 63 \end{matrix} \quad (46)$$

and hence possible for a representation 6 spin chain in general. The corresponding Casimirs are given by

$C_{\text{SU}(3)}^2(0;1) = \frac{4}{3}$, $C_{\text{SU}(3)}^2(2;0) = \frac{10}{3}$, and $C_{\text{SU}(3)}^2(1;2) = \frac{16}{3}$. This leads us to propose the parent Hamiltonian

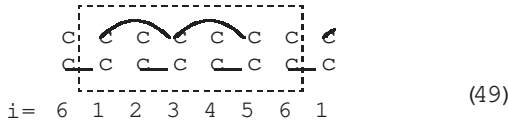
$$H_{6\text{VBS}} = \sum_{i=1}^N H_i \quad (47)$$

with

$$H_i = J_i^{(4)}{}^2 \frac{4}{3} + J_i^{(4)}{}^2 \frac{10}{3} + J_i^{(4)}{}^2 \frac{16}{3} : \quad (48)$$

Note that the operators J_i^a , $a = 1, \dots, 8$, are now given by 6×6 matrices, as the Gell-Mann matrices only provide the generators (9) of the fundamental representation 3. Since the representations 3, 6, and $\overline{15}$ possess the smallest Casimirs in the expansion (46), H_i and hence also $H_{6\text{VBS}}$ are positive semidefinite (i.e., have only non-negative eigenvalues). The three linearly independent states (45) are zero-energy eigenstates of (47).

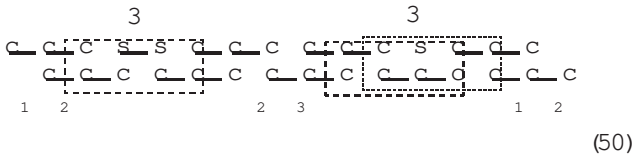
To verify that these are the only ground states, we have numerically diagonalized (47) for $N = 6$ and $N = 9$ sites. For $N = 9$, we find zero-energy ground states at momentum $k = 0; 3$; and 6 (in units of $\frac{2\pi}{N}$ with the lattice constant set to unity). Since the dimension of the Hilbert space required the use of a LANCZOS algorithm, we cannot be certain that there are no further ground states. We therefore diagonalized (47) for $N = 6$ as well, where we were able to obtain the full spectrum. We obtained five zero-energy ground states, two at momentum $k = 0$ and one each at $k = 2; 3; 4$. One of the ground states at $k = 0$ and the $k = 2; 4$ ground states constitute the space of momentum eigenstates obtained by Fourier transform of the space spanned by the three 6 VBS states (45). The remaining two states at $k = 0; 3$ are the momentum eigenstates formed by superposition of the state



(49)

and the same translated by one lattice spacing. It is readily seen that these two states are likewise zero energy eigenstates of (47) for $N = 6$ sites. The crucial difference, however, is that the 6 VBS states (45) remain zero-energy eigenstates of (47) for all N 's divisible by three, while the equivalent of (49) for larger N do not. We hence attribute these two additional ground states for $N = 6$ to the finite size, and conclude that the three states (45) are the only zero-energy ground states of (47) for general N 's divisible by three.

Excitations of the 6 VBS model are given by domain walls between two of the ground states (45). As in the trimer model, two distinct types of domain walls exist, which transform according to representations 3 and $\overline{3}$:



(50)

It is not clear which excitation has the lower energy, and it appears likely that both of them are stable against decay. Let us first look at the rep. 3 excitation. The four-site Hamiltonian (48) annihilates the state for all i 's except the four sites in the dashed box in (50), which contains the representations

$$\begin{array}{ccccccccc} 3 & 3 & 3 & 3 & 3 & & & & \\ = & 6 & 3 & 5 & 6 & \overline{15} & \overline{15} & 2 & 24 & \overline{42} \end{array}$$

i.e., the representations $\overline{15}^0 = (0;4)$, $24 = (3;1)$ twice, and $\overline{42} = (2;3)$ with Casimirs $\frac{28}{3}$, $\frac{25}{3}$ and $\frac{34}{3}$, respectively, in addition to representations annihilated by H_i . For the rep. 3 excitation sketched on the right in (50), there are two sets of four neighboring sites not annihilated by H_i as indicated by the dashed and the dotted box. Each set contains the representations

$$3 \quad 3 \quad 3 \quad 3 = 3 \quad 3 \quad 3 \quad 6 \quad 2 \quad \overline{15} \quad 24$$

i.e., only the rep. 24 in addition to representations annihilated by H_i . For our parent Hamiltonian (47), it hence may well be that the rep. 3 anti-coloron has the lower energy, but it is all but clear that the rep. 3 has sufficiently higher energy to decay. For general representation 6 spin chains, it may depend on the specifics of the model which excitation is lower in energy and whether the conjugate excitation decays or not.

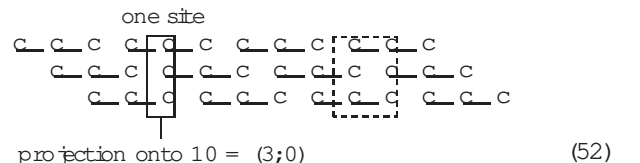
Since the excitations of the rep. 6 VBS chain are merely domain walls between different ground states, there is no confinement between them. We expect the generic antiferromagnetic rep. 6 chain to be gapless, even though the model we proposed here has a gap associated with the energy cost of creating a domain wall.

B. The representation 10 VBS

Let us now turn to the 10 VBS chain, which is a direct generalization of the AKLT chain to $\text{SU}(3)$. By combining the three different trimer states (43) for $i = 1; 2$; and 3 symmetrically,

$$\begin{aligned} |j_{10\text{VBS}}\rangle &= \frac{1}{\sqrt{3}} |b^y; r^y; g^y\rangle + \frac{2}{\sqrt{3}} |b^y; r^y; g^y\rangle + \frac{3}{\sqrt{3}} |b^y; r^y; g^y\rangle |j_0\rangle \\ &= \sum_i \sum_{(b;r;g)} \text{sign}(\cdot) \frac{Y_i}{i} \frac{Y_{i+1}}{i+1} \frac{Y_{i+2}}{i+2} |j_0\rangle; \quad (51) \end{aligned}$$

we automatically project out the rep. 10 in the decomposition $3 \times 3 \times 3 = 1 + 2 + 8 + 10$ generated on each lattice site by the three trimer chains. This construction yields a unique state, as illustrated:



(52)

In order to construct a parent Hamiltonian, note first that the total spin on two (neighboring) sites of a rep. 10 chain is given by

$$\overline{10} \otimes \overline{10} = \overline{10} \oplus 27 \oplus 28 \oplus 35; \quad (53)$$

On the other hand, the total spin of two neighboring sites for the 10 VBS state can contain only the representations

$$3 \oplus 3 \oplus 3 \oplus 3 = 2 \oplus 1 \oplus 4 \oplus 8 \oplus \overline{10} \oplus 27; \quad (54)$$

as can be seen easily from the dashed box in the cartoon above. (Note that this result is independent of how many sites we include in the dashed box.) After the projection onto rep. 10 on each lattice site, we find that only reps. $\overline{10} = (0;3)$ and $27 = (2;2)$ occur for the total spin of two neighboring sites for the 10 VBS state. With the Casimirs $C_{SU(3)}^2(0;3) = 6$ and $C_{SU(3)}^2(2;2) = 8$ we obtain the parent Hamiltonian

$$H_{10VBS} = \sum_{i=1}^N J_i J_{i+1}^2 + 5 \sum_{i=1}^N J_i J_{i+1} + 6N; \quad (55)$$

the operators J_i^a , $a = 1, \dots, 8$, are now 10×10 matrices, and we have used $J_i^2 = 6$. H_{10VBS} is positive semidefinite and annihilates the 10 VBS state (51). We assume that (51) is the only ground state of (55).

The Hamiltonian (55) provides the equivalent of the AKLT model [15, 16], whose unique ground state is constructed from dimer states by projection onto spin 1, for $SU(3)$ spin chains. Note that as in the case of $SU(2)$, it is sufficient to consider linear and quadratic powers of the total spin of only two neighboring sites. This is a general feature of the corresponding $SU(n)$ models, as we will elaborate in the following section.

Since the 10 VBS state (51) is unique, we cannot have domain walls connecting different ground states. We hence expect the coloron and anti-coloron excitations to be confined in pairs, as illustrated below. The state between the excitations is no longer annihilated by (55), as there are pairs of neighboring sites containing higher-dimensional representations, as indicated by the dotted box below. As the number of such pairs increases linearly with the distance between the excitation, the confinement potential depends linearly on this distance.

coloron

3

anti-coloron

3

energy cost / distance

(56)

In principle, it would also be possible to create three colorons (or three anti-colorons) rather than a coloron (anti-coloron) pair, but as all three excitations would feel strong confinement forces, we expect the coloron (anti-coloron) pair to constitute the dominant low energy excitation. The confinement force between the pair induces a linear

oscillator potential for the relative motion of the constituents. The zero-point energy of this oscillator gives rise to a Haldane-type energy gap (see [71, 72] for a similar discussion in the two-leg Heisenberg ladder), which is independent of the model specifics. We expect this gap to be a generic feature of rep. 10 spin chains with short-range antiferromagnetic interactions.

C. The representation 8 VBS

To construct a representation 8 VBS state, consider first a chain with alternating representations 3 and $\bar{3}$ on neighboring sites, which we combine into singlets. This can be done in two ways, yielding the two states

$$\begin{array}{c} c \\ \hline e \end{array} \begin{array}{c} c \\ \hline e \end{array} \begin{array}{c} c \\ \hline e \end{array} \quad \text{and} \quad \begin{array}{c} c \\ \hline e \end{array} \begin{array}{c} e \\ \hline c \end{array} \begin{array}{c} e \\ \hline c \end{array} \begin{array}{c} e \\ \hline c \end{array}.$$

3 3

We then combine a $3\bar{3}$ state with an identical one shifted by one lattice spacing. This yields representations $3 \oplus \bar{3} = 1 \oplus 8$ at each site. The 8 VBS state is obtained by projecting onto representation 8. Corresponding to the two $3\bar{3}$ states illustrated above, we obtain two linearly independent 8 VBS states, L and R , which may be visualized as

one site

projection onto 8 = (1;1)

(57)

These states transform into each other under space reflection or color conjugation (interchange of 3 and $\bar{3}$).

It is convenient to formulate the corresponding state vectors as a matrix product. Taking (b, r, g) and $(\bar{y}, \bar{c}, \bar{m})$ as bases for the reps. 3 and $\bar{3}$, respectively, the singlet bonds in L above can be written

$$\begin{aligned} & b_i \bar{y}_{i+1} + r_i \bar{c}_{i+1} + g_i \bar{m}_{i+1} \\ &= \begin{pmatrix} 0 & 1 \\ b_i & r_i & g_i \end{pmatrix} \begin{pmatrix} \bar{y}_{i+1} \\ \bar{c}_{i+1} \\ \bar{m}_{i+1} \end{pmatrix} \end{aligned}$$

We are hence led to consider matrices composed of the outer product of these vectors on each lattice site,

$$M_i^{18} = \begin{pmatrix} 0 & 1 \\ b_i & r_i & g_i \end{pmatrix} \begin{pmatrix} \bar{y}_i \\ \bar{c}_i \\ \bar{m}_i \end{pmatrix}$$

In the case of the AKLT model reviewed above, the Schwinger bosons take care of the projection automatically, and we can simply assemble these matrices into a product state. For the 8 VBS, however, we need to enforce the projection explicitly. This is most elegantly

accomplished using the Gell-Mann matrices, yielding the projected matrix

$$M_i = \frac{1}{2} \sum_{a=1}^8 \text{tr} (M_i^a X^a) : \quad (58)$$

Here we have simply used the fact that the eight Gell-

Mann matrices, supplemented by the unitary matrix, constitute a complete basis for the space of all complex 3×3 matrices. By omitting the unit matrix in the expansion (58), we effectively project out the singlet state. Written out explicitly, we obtain

$$M_i = \begin{pmatrix} 0 & \frac{2}{3} \text{by}_i & \frac{1}{3} \text{jci}_i & \frac{1}{3} \text{jmi}_i & \text{jyi}_i & \text{by}_i & 1 \\ \frac{2}{3} \text{by}_i & 0 & \text{bci}_i & \frac{1}{3} \text{by}_i + \frac{2}{3} \text{jci}_i & \frac{1}{3} \text{jmi}_i & \text{jci}_i & 0 \\ \frac{1}{3} \text{jci}_i & \text{bci}_i & 0 & \text{jmi}_i & \text{jmi}_i & \frac{1}{3} \text{by}_i & \frac{1}{3} \text{jci}_i + \frac{2}{3} \text{jmi}_i \\ \frac{1}{3} \text{jmi}_i & \frac{1}{3} \text{by}_i + \frac{2}{3} \text{jci}_i & \text{jmi}_i & 0 & \text{jyi}_i & \text{by}_i & 0 \\ \text{jyi}_i & \text{by}_i & \text{jmi}_i & \text{jci}_i & 0 & 0 & 0 \\ \text{by}_i & \text{jci}_i & \frac{1}{3} \text{by}_i + \frac{2}{3} \text{jmi}_i & \text{jci}_i & \text{by}_i & 0 & 0 \\ 1 & 0 & \frac{1}{3} \text{jci}_i + \frac{2}{3} \text{jmi}_i & 0 & 0 & 0 & 0 \end{pmatrix} : \quad (59)$$

Assuming PBCs, the 8 VBS state L (illustrated in on the left (57)) is hence given by the trace of the matrix product

$$^L_{8\text{VBS}} = \text{tr}_i^Y M_i : \quad (60)$$

To obtain the state R (illustrated on the right in (57)) we simply have to transpose the matrices in the product,

$$^R_{8\text{VBS}} = \text{tr}_i^Y M_i^T : \quad (61)$$

Let us now formulate a parent Hamiltonian for these states. If we consider two lattice sites on an $SU(3)$ chain with a representation 8 on each lattice site in general, we find the full $SU(3)$ content

$$8 \otimes 8 = 1 \oplus 2 \oplus 8 \oplus 10 \oplus \overline{10} \oplus 27 \quad (62)$$

with $10 = (3;0)$, $\overline{10} = (0;3)$, and $27 = (2;2)$. On the other hand, for the 8 VBS states only the representations $3 \otimes 3 = 1 \oplus 8$ can occur for the total spin of two neighboring sites, as the two sites always contain one singlet (see dashed box in (57) on the right above). With the Casimirs $C_{SU(3)}^2(0;0) = 0$ and $C_{SU(3)}^2(1;1) = 3$ for representations 1 and 8, respectively, we construct the parent Hamiltonian

$$H_{8\text{VBS}} = \sum_{i=1}^N J_i J_{i+1}^2 + \frac{9}{2} J_i J_{i+1} + \frac{9}{2} ; \quad (63)$$

where the operators J_i^a , $a = 1; \dots; 8$, are now 8×8 matrices, and we have used the Casimir $J_i^2 = 3$ on each site. $H_{8\text{VBS}}$ is positive semidefinite, and annihilates the states L and R . We have numerically verified for chains with $N = 3, 4, 5$, and 6 lattice sites that L and R are the only ground states of (63).

Naively, one might assume the 8 VBS model to support deconfined spinons or colorons, which correspond to domain walls between the two ground states L and R . A

closer look at the domain walls, however, shows that this is highly unlikely, as each domain wall is a bound state of either two anti-colorons or two colorons, as illustrated below.

$$\begin{array}{ccccc} \text{anti-colorons} & & & & \text{colorons} \\ & 3 & 3 & & 3 & 3 \\ \text{c} & \text{e} & \text{c} & \text{e} & \text{s} & \text{e} & \text{c} & \text{e} & \text{c} & \text{e} & \text{c} & \text{e} & \text{c} & \text{e} \\ \text{c} & \text{e} & \text{s} & \text{e} & \text{c} & \text{e} & \text{c} & \text{e} & \text{c} & \text{e} & \text{c} & \text{e} & \text{c} & \text{e} \\ L & & & & R & & & & L \end{array} \quad (64)$$

There is no reason to assume that the domain wall depicted above as two anti-colorons in fact corresponds to a single coloron, as it appears to be the case for the trimer chain. There we created a domain wall corresponding to a single coloron by removing one of the rep. 3 spins from a trimer, leaving the remaining rep. 3 spins coupled antisymmetrically as in the ground state. If we were to combine the two reps. 3 into a rep. 3 in (64), we would not reproduce a correlation present in the ground state, but enforce a new correlation. The correct interpretation of the domain wall between L and R is hence that of a bound state between two linearly confined anti-colorons. The origin of the confining potential is illustrated below.

$$\begin{array}{ccccc} \text{anti-coloron} & & & & \text{anti-coloron} \\ & 3 & & & 3 \\ \text{c} & \text{e} & \text{c} & \text{e} & \text{c} & \text{e} & \text{s} & \text{e} & \text{c} \\ \text{c} & \text{e} & \text{s} & \text{e} & \text{c} & \text{e} & \text{c} & \text{e} & \text{c} \\ L & & & & R \end{array}$$

energy cost / distance

(65)

As in the 10 VBS, the confinement induces a linear oscillator potential for the relative motion of the anti-colorons. The zero-point energy of this oscillator corresponds to a Haldane-type gap in the spectrum. The ground state wave function of the oscillator is symmetric, and hence corresponds to a symmetric combination of $3 \otimes 3$, i.e., rep. 6. The antisymmetric combination of $3 \otimes 3$ corresponds to the first excited state of the oscillator,

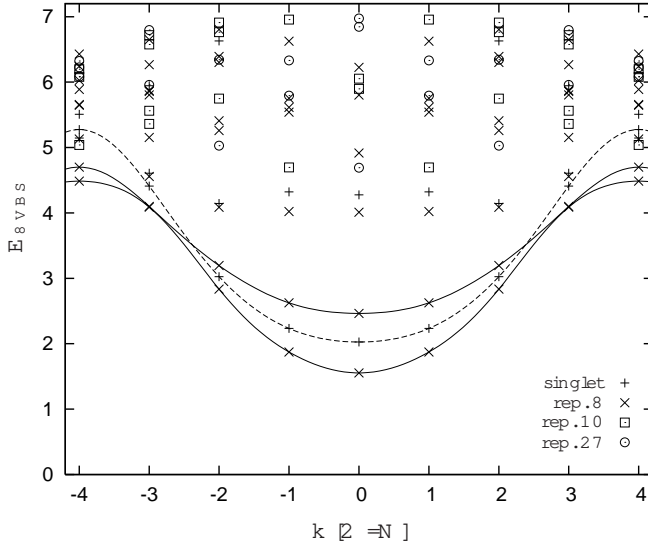


FIG. 14: Spectrum of the 8 VBS Hamiltonian (63) for $N = 8$ sites obtained by exact diagonalization. (The lines are merely guides to the eye.) The "magnon" excitation transforming under rep. 8 of $SU(3)$ has the lowest energy, followed by a singlet excitation, as expected from the discussion in the text. The well defined modes at low energies provide strong evidence of coloron (anti-coloron) bound states as compared to deconfined domain walls, and hence support our conclusion that the 8 VBS exhibits a Haldane gap due to spinon confinement.

which we expect to cost more than twice the energy of the symmetric state [72]. This statement holds for the pair of colorons in (64) as well.

The domain walls, however, are not the only low energy excitations. In either of the ground states, we can create coloron (anti-coloron) bound states, which make no reference to the other ground state, as illustrated below.

$$\begin{array}{ccccccc}
 & \text{anti-coloron} & & & \text{coloron} & & \\
 & 3 & & & 3 & & \\
 \text{c} & \text{e} & \text{c} & \text{e} & \text{c} & \text{e} & \text{c} \\
 \text{c} & \text{e} & \text{s} & \text{e} & \text{c} & \text{e} & \text{c} \\
 \text{L} & & & & & & \text{L} \\
 & \text{energy cost / distance} & & & & &
 \end{array} \quad (66)$$

The oscillator model tells us again that the "symmetric" combination of $3 \oplus 3$, i.e., rep. 8, has the lowest energy, which we expect to be comparable, if not identical, to the energy required to create each of the domain walls above. The singlet will have an energy comparable to that of a domain wall transforming under either 3 or $\bar{3}$. In any event, we expect the 8 VBS model to display a Haldane gap due to coloron confinement.

The excitation spectrum of (63) for a chain with $N = 8$ sites and PBCs is shown in Fig. 14. The spectrum shows that the lowest excitation transforms under rep. 8, as expected from (66), with a singlet and then another rep. 8 following at slightly higher energies. It is tempting to interpret those three levels as the lowest levels of

the coloron (anti-coloron) oscillator (66), but then there should be another singlet at a comparable spacing above. The fact that the spacings between these excitations are significantly smaller than the energy of the first excited state, however, would be consistent with such an interpretation, as the spinons in VBS models always have a local energy cost associated with their creation, which is specific to these models and not related to the universal Haldane gap stemming from confinement forces.

Most importantly, the spectrum provides strong evidence in favor of our assumption that the domain walls are not elementary excitations, but bound states of either two colorons or two anti-colorons, and hence that the lowest energy excitations of finite chains are coloron (anti-coloron) bound states as illustrated in (66). The assumption is crucial for our conclusion that the model exhibits a Haldane gap. If the low energy sector of the model was determined by two deconfined domain walls, we would see a continuum of states in the spectrum, similar to the spectrum seen in spin $S = \frac{1}{2}$ chains of $SU(2)$. The well defined low-energy modes in Fig. 14, however, look much more like the spinon (spinon bound state) excitations seen in $S = 1$ chains or two-leg $S = \frac{1}{2}$ Heisenberg ladders. In particular, if we assume that the individual domain walls transform under reps. 6 and $\bar{6}$, we expect excitations transforming under the representations contained in $6 \otimes \bar{6} = 1 \oplus 8 \oplus 27$ to be approximately degenerate. Fig. 14 shows clearly that such a multiplet is not present at the lowest energies.

IX. $SU(n)$ MODELS

In this section, we generalize three of the models proposed for $SU(3)$ spin chains, the trimers model, the symmetric representation 10 VBS, and the matrix product state 8 VBS to the case of $SU(n)$ spin chains.

A. The trimer model

Consider an $SU(n)$ spin chain with N sites, where N is a multiple of n , with a spin transforming according to the fundamental representation n of $SU(n)$ at each lattice site,

$$n = (1; 0; \dots; 0) = \square \triangleq c^y j 0 i; \quad (67)$$

where \square denotes a "avor", $2 \leq f_1, \dots, f_n$, and c^y creates a fermion of avor y .

The $SU(n)$ generators at site i are in analogy to (3) and (9) defined as

$$J_i^a = \frac{1}{2} \sum_{y=0}^{n-1} c_1^y V^a c_1^y; \quad a = 1; \dots; n^2 - 1; \quad (68)$$

where the V^a denote the $n^2 - 1$ $SU(n)$ Gell-Mann matrices [73]. The generators are normalized through the

On the other hand, the total $SU(n)$ spin of two neighboring sites of the representation $(n; 0; \dots; 0)$ VBS (74) has to be contained in the product

$$\begin{array}{|c|} \hline n-1 \\ \hline \end{array} \quad \square \quad \square \quad (76)$$

As we project the spin on each lattice site onto the representation $(n; 0; \dots; 0)$, only two these representations remain:

$$\begin{array}{|c|c|c|c|} \hline & & & \\ \hline & & & \\ \hline \end{array} \quad \text{and} \quad \begin{array}{|c|c|c|c|} \hline & & & \\ \hline & & & \\ \hline \end{array}$$

The eigenvalues of the quadratic Casimir operator are given by $g_n(0) = 2n(n-2)$ and $g_n(1) = 2(n-1)^2$, respectively. Hence, using $J_i^2 = n(n-1)$, we obtain the parent Hamiltonian

$$H_{(n; 0; \dots; 0) \text{ VBS}} = \sum_{i=1}^N J_i J_{i+1}^2 + (2n-1) J_i J_{i+1} + n(n-1) : \quad (77)$$

Since $g_n(0) = 0$ for $n = 2$ and $g_n(\cdot)$ is a strictly increasing function of \cdot , the Hamiltonian (77) is positive semidefinite. For $n = 2$, we recover the AKLT model (40); for $n = 3$, we recover the 10 VBS model (55).

C. An example of a matrix product state

In principle, a matrix product VBS can be formulated on all $SU(n)$ chains with spins transforming under the symmetric combination of any representation m and its conjugate representation \bar{m} . Unless the rep. m is self-conjugate, we obtain two inequivalent states, which transform into each other under space reflection. The construction of these is analogous to the 8 VBS introduced above, and likewise best illustrated as

$$\begin{array}{c} \text{one site} \\ \begin{array}{c} m \text{---} \bar{m} \quad m \text{---} \bar{m} \quad m \text{---} \bar{m} \\ \text{---} \bar{m} \quad \text{---} \bar{m} \quad \text{---} \bar{m} \end{array} \quad \text{and} \quad \begin{array}{c} \boxed{m \text{---} \bar{m}} \text{---} m \\ \boxed{\bar{m} \text{---} m} \end{array} \\ \text{projection onto the symmetric} \\ \text{combination in } m \text{---} \bar{m} \end{array} \quad (78)$$

The thick lines indicate that we combine pairs of neighboring representations m and \bar{m} into singlets. On each lattice site, we project onto the symmetric combination of m and \bar{m} , as indicated. By "symmetric combination" we mean that if representations m and \bar{m} of $SU(n)$ have Dynkin coordinates $(\lambda_1; \lambda_2; \dots; \lambda_{n-1})$ and $(\lambda_{n-1}; \lambda_{n-2}; \dots; \lambda_1)$, respectively, we combine them into the representation with Dynkin coordinates $(\lambda_1 + \lambda_{n-1}; \lambda_2 + \lambda_{n-2}; \dots; \lambda_{n-1} + \lambda_1)$. In other words, we align the columns of both tableaux horizontally, and hence obtain a tableau with twice the width, without ever adding

a single box vertically to a column n of the tableaux we started with. The states (78) we obtain are translationally invariant and we expect the parent Hamiltonians to involve nearest-neighbor interactions only.

In this subsection, we will formulate the simplest $SU(n)$ model of this general family. We take m to be the representation formed by antisymmetrically combining $\frac{n}{2}$ fundamental representations,

$$m = \left[\begin{array}{|c|} \hline (0; \dots; 0; 1; 0; \dots; 0) \\ \hline \end{array} \right] = \begin{array}{|c|} \hline \\ \hline \end{array} \quad \text{boxes,} \\ \text{1-th entry}$$

which implies that we consider a model with the representation corresponding to a Young tableaux with a column n with n boxes to the left of a column n with n boxes at each lattice site:

$$\left[\begin{array}{|c|} \hline \\ \hline \end{array} ; n \right] = \begin{array}{|c|} \hline \\ \hline \end{array} \quad \text{rows}$$

The construction of the parent Hamiltonian is similar to the n -mer model above. The total spin on two neighboring lattice sites can only assume representations contained in $m \otimes \bar{m}$, i.e., representations corresponding to tableaux of the form

$$\left[\begin{array}{|c|} \hline \\ \hline \end{array} ; n \right] = \begin{array}{|c|} \hline \\ \hline \end{array} \quad \text{rows}$$

with $0 \leq b \leq n$. The eigenvalues of the quadratic Casimir operator for these representations are

$$h_n(b) = (n-b+1) : \quad (79)$$

The obvious proposal for a parent Hamiltonian is hence

$$H = \sum_{i=1}^N H_i; \quad H_i = \sum_{b=0}^{b_{\text{max}}} J_i^{(2)} h_n(b) : \quad (80)$$

where b_{max} denotes again the floor function. This Hamiltonian singles out the matrix product state (78) as unique ground states for $n = 5$, but suffers from the same shortcomings as (71) with (72) for $n = 6$.

X. SPIN ON CONFINEMENT AND THE HALDANE GAP

A. The Alicki-Lieb theorem

For the generic $SU(2)$ spin chain, Haldane [8, 9] identified the $O(3)$ nonlinear sigma model as the effective low

energy field theory of SU(2) spin chains, and argued that chains with integer spin possess a gap in the excitation spectrum, while a topological term renders half-integer spin chains gapless [10, 11]. The exact models for SU(2) spin chains we reviewed above, the M G and the AKLT chain, serve as paradigms to illustrate the general principle. Unfortunately, the effective field theory description of Haldane yielding the distinction between gapless half-integer spin chains with deconfined spinons and gapped integer spin chains with confined spinons cannot be directly generalized to SU(n) chains, as there is no direct equivalent of the CP^1 representation used in Haldane's analysis.

Nonetheless, there is a rigorous and rather general result for antiferromagnetic chains of SU(n) spins transforming under a representation corresponding to a Young tableau with a number of boxes not divisible by n: Affeck and Lieb [63] showed that if the ground state is non-degenerate, and the Hamiltonian consists of nearest-neighbor interactions only, then the gap in the excitation spectrum vanishes as $1/N$ (where N is the number of sites) in the thermodynamic limit. This result is fully consistent with the picture suggested by the models introduced above. Like the M G model, the trim er model and the representation 6 VBS have degenerate ground states and interactions which extend beyond the nearest neighbor, which implies that the theorem is not directly applicable.

On physical grounds, however, the statement that a given model is gapless (i.e., the excitation gap vanishes in the thermodynamic limit) implies that the spinons are deconfined. The reason is simply that if there was a confinement force between them, the zero-point energy associated with the quantum mechanical oscillator of the relative motion between the spinons would inevitably yield an energy gap. The M G, the trim er and the 6 VBS model constitute pedagogically valuable paradigms of deconfined spinons. Since the excitations in these models are literally domain walls between different ground states, no long-range forces can exist between them.

B. A general criterion for spinon confinement

More importantly, however, the exact models we introduced above provide information about the models of SU(n) spin chains with representations corresponding to Young tableaux with a number of boxes divisible by n, i.e., models for which the Affeck-Lieb theorem is not applicable. We have studied two SU(3) models belonging to this family in Sec. VIII, the rep. 10 VBS and the rep. 8 VBS, and found that both have confined spinons or colorons and hence display a Haldane-type gap in the spectrum.

In this section, we will argue that models of antiferromagnetic chains of SU(n) spins transforming under a representation corresponding to a Young tableau consisting of a number of boxes divisible by n generally possess

a Haldane-type gap due to spinon confinement forces.

We should caution immediately that our argument is based on several assumptions, which we consider reasonable, but which we are ultimately unable to prove.

The first, and also the most crucial, is the assumption that the question of whether a given model supports free spinon excitations can be resolved through study of the corresponding VBS state. This assumption definitely holds for SU(2) spin chains, where the M G model for $S = \frac{1}{2}$ indicates that the spinons are free, while the AKLT model for $S = 1$ serves as a paradigm for spinon confinement and hence the Haldane gap. The general conclusions we derived from our studies of the SU(3) VBSs above rely on this assumption. The numerical results we reported on the rep. 8 VBS provide evidence that this assumption holds at least for this model.

Let us consider an SU(n) spin chain with spins transforming under a representation corresponding to Young tableau consisting of L columns with $\lambda_1 \lambda_2 \dots \lambda_L$ $\lambda_L < n$ boxes each,

$$[\lambda_1; \lambda_2; \dots; \lambda_L] \quad (81)$$

with a total number of boxes

$$\sum_{i=1}^L \lambda_i = L$$

divisible by n. We denote the Dynkin coordinates of this representation by $(\lambda_1; \lambda_2; \dots; \lambda_{n-1})$, which implies

$$\sum_{i=1}^{n-1} \lambda_i = L$$

Note that this representation is, by definition, given by the maximally symmetric component of the tensor product of the individual columns,

$$[\lambda_1; \lambda_2; \dots; \lambda_L] = S[\lambda_1] \otimes [\lambda_2] \otimes \dots \otimes [\lambda_L] \quad (82)$$

For convenience, we denote the n -dimensional representation $[\lambda]$ in this subsection as $\chi_\lambda = \chi^\dagger_\lambda$.

Since L is divisible by n, it will always be possible to obtain a singlet from the complete sequence of representations $\chi_{\lambda_1}; \chi_{\lambda_2}; \dots; \chi_{\lambda_L}$ by combining them antisymmetrically. To be precise, when we write that we combine representations χ_{λ_1} and χ_{λ_2} antisymmetrically, we mean we obtain a new representation $[\lambda_1 + \lambda_2]$ by stacking the two columns with λ_1 and λ_2 boxes on top of each other if $\lambda_1 + \lambda_2 < n$, and a new representation $[\lambda_1 + \lambda_2 - n]$ if $\lambda_1 + \lambda_2 \geq n$. In equations, we write this as

$$A[\lambda_1] \otimes [\lambda_2] = \begin{cases} [\lambda_1 + \lambda_2] & \text{for } \lambda_1 + \lambda_2 < n \\ [\lambda_1 + \lambda_2 - n] & \text{for } \lambda_1 + \lambda_2 \geq n \end{cases} \quad (83)$$

Following the notation used above, we indicate the antisymmetric combination of representations λ_1 by a line connecting them. In particular, we depict the singlet formed by combining $\lambda_1; \lambda_2; \dots; \lambda_L$ on different lattice sites as

$$\lambda_1^i \text{---} \lambda_2^i \text{---} \lambda_3^i \text{---} \dots \text{---} \lambda_L^i \quad (84)$$

The understanding here is that we combine them in the order indicated by the line, i.e., in (84) we first combine λ_1 and λ_2 , then we combine the result with λ_3 , and so on. Depending on the order of the representations λ_1 on the line, we obtain different, but not necessarily orthogonal, singlets. We assume that it is irrelevant whether we combine the representations starting from the left or from the right of the line, as the resulting state will not depend on it.

In general, it will be possible to construct a number ϕ_n of singlets out of various combinations of the λ_i 's, one for each block of λ_i 's for which the values of ϕ add up to n as we combine the representation in the order described above. In this case, we will be able to construct one VBS for each singlet, and subsequently combine them at each site symmetrically to obtain the desired representation (81). The argument for spinon confinement we construct below will hold for each of the individual VBSs, and hence for the combined VBS as well. It is hence sufficient for our purposes to consider situations where the entire sequence $\lambda_1; \lambda_2; \dots; \lambda_L$ is needed to construct a singlet.

A possible VBS "ground state" for a representation corresponding to a Young tableau with $L = 4$ columns is depicted below.

one site

projection onto representation $[1; 2; 3; 4]$ (85)

In general, there are as many inequivalent VBS "ground states" as there are inequivalent ways to order the representations $\lambda_1; \lambda_2; \dots; \lambda_L$, i.e., the number of inequivalent VBS "ground states" is given by

$$\frac{L!}{1! \ 2! \ \dots \ n! \ 1!}.$$

To give an example, the following VBS

one site

projection onto representation $[1; 2; 3; 4]$ (86)

is inequivalent to the one above if and only if $\lambda_1 \notin \lambda_2$. Note that all these VBS "ground states" are translationally invariant. We expect some of these states, but not all of them, degenerate in energy for the appropriate parent Hamiltonian, and have accordingly written "ground states" in quotation marks. For example, if we form a $SU(4)$ VBS with representation $[\lambda_1; \lambda_2; \lambda_3] = [1; 1; 2]$, the combination

$$\lambda_1^i \text{---} \lambda_3^i \text{---} \lambda_2^i$$

might yield a state with a lower energy for the appropriate Hamiltonian than the state formed by combining

$$\lambda_1^i \text{---} \lambda_2^i \text{---} \lambda_3^i :$$

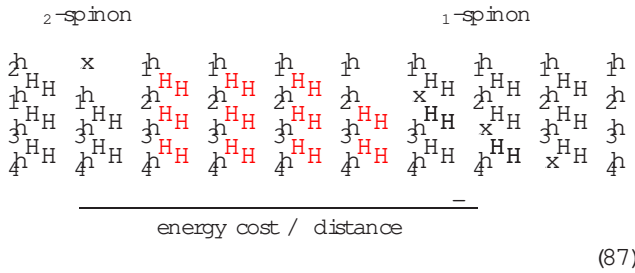
Simple examples where we have only two inequivalent VBS ground states are provided by the matrix product states discussed in Secs. VIII C and IX C.

We will now argue that the elementary excitations of the corresponding VBS models are always confined. To this end, we first observe that any domain wall between translationally invariant "ground states" consists of a total of m n representations λ_1 (m integer). To illustrate this, consider a domain wall between the "ground states" depicted in (86) and (85):

In the example, the domain wall consists of reps. λ_2 , λ_2 , λ_3 , and λ_4 . If the translationally invariant states on both sites are true ground states, the domain wall is likely to correspond to two elementary excitations: a rep. λ_1 spinon consisting of an antisymmetric combination of a λ_2 , a λ_3 , and a λ_4 , as indicated by the line in the drawing, and another rep. λ_2 spinon. The reason we assume that λ_2 , λ_3 , and λ_4 form a rep. λ_1 is simply that this combination is present in both ground states on either side, and hence bound to be the energetically most favorable combination. The second λ_2 , however, is not part of this elementary excitation, as combining it antisymmetrically with the others (i.e., the λ_1) would induce correlations which are not present in the ground state. We hence conclude that the second λ_2 is an elementary excitation as well. The domain wall depicted above consists of a spinon transforming under rep. λ_1 and an anti-spinon transforming under rep. λ_2 .

The next step in our argument is to notice that the spinon and the complementary particle created simultaneously which may either be its anti-particle or some other spinon, are confined through a linear potential. To see this, we pull them apart and look at the state inbe-

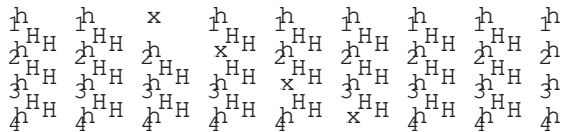
tween (color online):



The state between spinon and anti-spinon is not translationally invariant. In the example, the unit cell of this state is depicted in red and consists of two regular bonds with three "singlet lines" between the sites, one stronger bond with four lines (which cross in the cartoon), and one weaker bond with only two lines. If we assume that the two states (86) and (85) on both sides are true ground states, it is clear that the irregularities in the strength of the bond correlations will cause the state between the spinon and anti-spinon to have a higher energy than either of them. This additional energy cost will induce a linear confinement potential between the spinons, and hence a linear oscillator potential for the relative motion of the particles. As in the models studied above, the Haldane gap corresponds to the zero-point energy of this oscillator.

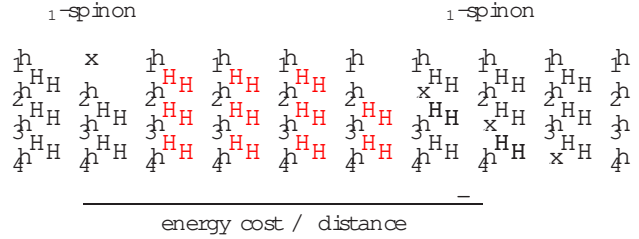
If one of the "ground states" to the left or to the right of the domain wall is not a true ground state, but a translationally invariant state corresponding to a higher energy than the ground state, there will be a confining force between this domain wall and another domain wall which transforms the intermediate "ground state" with a higher energy back into a true ground state. This force will be sufficient to account for a Haldane gap, regardless of the strength or existence of a confinement force between the constituent particles of each domain wall.

The lowest-lying excitations of a representation $[1; 2; \dots; L]$ spin chain, however, will in general not be domain walls, but spinons created by breaking up one of the singlets (84) in a ground state. This is illustrated below for the ground state (85):



In the example, we have created a spinon transforming under rep._1 and its anti-particle, a spinon transforming under rep._1 . This is, however, irrelevant to the argument: we may break the singlet in any way we like. The important feature is that we obtain, by construction, at least two excitations, and that these are confined. In our specific example, the confinement potential is equivalent

to the confinement potential in (87) above (color online):



We leave it to the reader to convince him – or herself – that the conclusions regarding confinement drawn from the simple examples studied here hold in general.

C. Models with confinement through interactions extending beyond nearest neighbors

Let us briefly summarize the results obtained. The $SU(n)$ models we have studied so far fall into two categories. The models belonging to the first – the trimers chain, the 6 VBS, and the n -mer chain – have n degenerate ground states, which break translational invariance up to translations by n lattice spacings. The Young tableaux describing the representations of $SU(n)$ at each site consist of a number of boxes which is smaller than n , and hence obviously not divisible by n . The models support deconfined spinon excitations, and hence do not possess a Haldane gap in the spectrum. The Hamiltonians of these models require interactions between $n + 1$ neighboring sites along the chain. Even though the Alicki-Lieb theorem is not directly applicable to the models we constructed above, it is applicable to $SU(n)$ spin chains with spins transforming under the same representations. Like the VBS models, the theorem suggests that there is no Haldane gap in this family of models.

The models belonging to the second category – the 10 VBS, the 8 VBS, the representation $(n; 0; \dots; 0)$ VBS, and the \bar{m} -matrix product state – have translationally invariant ground states. The ground states are unique for some models, like the 10 and the $(n; 0; \dots; 0)$ VBS, and degenerate for others, like the 8 VBS. The Young tableaux describing the representations of $SU(n)$ at each site consist of a number of boxes which is divisible by n . The Alicki-Lieb theorem is not applicable to models of this category. The spinon excitations for this category of models are subject to confinement forces, which give rise to a Haldane gap. The parent Hamiltonians for these models require interactions between nearest-neighbor sites only.

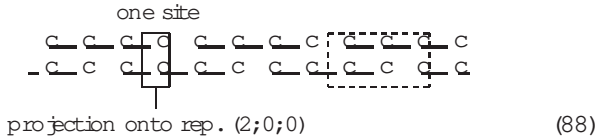
At first glance, this classification might appear complete. Further possibilities arise, however, in $SU(n)$ spin chains where number of boxes in the Young tableau consists of n and n have a common divisor different from n , which obviously requires that n is not a prime number. In this case, it is possible to construct VBS models in which the ground state breaks translational invariance

only up to translations by $n=q$ lattice spacings, where q denotes the largest common divisor of n and n such that $q < n$. This implies that the ground state of the appropriate, translationally invariant Hamiltonian will be $n=q$ -fold degenerate. In the examples we will elaborate on below, the parent Hamiltonians for these models require interactions between $\frac{n}{q} + 1$ sites, a feature we conjecture to hold in general. The spinon excitations of these models are connected, even though the Alicki-Lieb theorem states that the nearest-neighbor Heisenberg chain of $SU(n)$ spins transforming under these representations is gapless. (We implicitly assume here that the ground states of the $SU(n)$ nearest-neighbor Heisenberg chains are non-degenerate.) Let us illustrate the general features of this third category of models with a few simple examples.

(1) Consider an $SU(4)$ chain with spins transforming under the 10-dimensional representation

$$(2;0;0) = \square\square :$$

Following the construction principle of the 6 VBS of $SU(3)$, we find that the two degenerate VBS states illustrated through



(88)

are exact zero-energy ground states of

$$H_{(2;0;0) \text{ VBS}} = \sum_{i=1}^N J_i^{(3)}{}^4 - 12 \sum_{i=1}^N J_i^{(3)}{}^2 + \frac{135}{4} ; \quad (89)$$

which contains next-nearest neighbor interactions.

The example illustrates the general rule stated above. The largest common divisor of $n = 4$ and $n = 2$ is $q = 2$. This implies $\frac{n}{q} = 2$ and hence two degenerate VBS states which break translational invariance up to translations by two lattice spacings. The parent Hamiltonian requires interaction between three neighboring sites.

According to the Alicki-Lieb theorem, models of antiferromagnetic $SU(4)$ chains of representation $(2;0;0)$ with nearest-neighbor Heisenberg interactions and non-degenerate ground states are gapless in the thermodynamic limit, which implies that the spinons are deconfined. In all the models we have studied in previous sections, the conclusions drawn from the Alicki-Lieb theorem were consistent with those drawn from our exact models. For the present model, however, they are not consistent.

Specifically, we strongly conjecture that the spinons in the $(2;0;0)$ VBS are connected. This conjecture is based on the reasonable assumption that the elementary excitations of the model transform as either the fundamental representation $4 = (1;0;0)$ of $SU(4)$ or its conjugate representation $\bar{4} = (0;0;1)$. This assumption implies that

a single domain wall in one of the 4-mer chains used to construct the VBS state (88) shifts this chain by one lattice spacing. If we assume a ground state to the left of the spinon, the state on to the right will have a higher energy for the next-nearest neighbor Hamiltonian (89), as illustrated below.



(90)

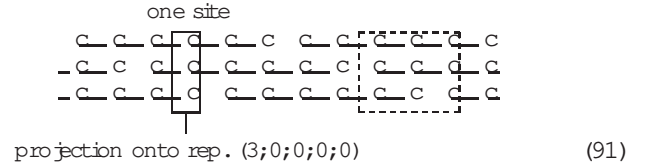
To recover the ground state, a second domain wall is required nearby, which is bound to the first by a linear potential.

Our conclusion is not in contradiction with the rigorous result of Alicki and Lieb, as they explicitly restrict themselves to models with nearest-neighbor interactions. If we had only nearest-neighbor interactions, the energy expectation value in the region between the domain walls would not be higher than in the ground state, as one can see easily from the cartoon above: the sequence of alternating links would merely shift from (strong, weak, strong, weak) to (strong, strong, weak, weak).

(2) The situation is similar for an $SU(6)$ chain with spins transforming under the 56-dimensional representation

$$(3;0;0;0;0) = \square\square\square :$$

With $n = 6$ and $n = 3$, we have again $\frac{n}{q} = 2$. Accordingly, we find that the two VBS states illustrated through



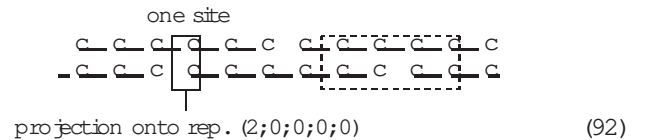
(91)

are exact ground states of a parent Hamiltonian containing up to next-nearest-neighbor interactions only, and that the spinon excitations are connected.

(3) As a third example, consider an $SU(6)$ spin chain with spins transforming under the 21-dimensional representation

$$(2;0;0;0;0) = \square\square :$$

This implies $\frac{n}{q} = 3$. We find that the three VBS states illustrated by



(92)

are exact ground states of a parent Hamiltonian involving the quadratic Casimir of total spin of four neighboring

sites,

$$H_{(2;0;0;0) \text{ VBS}} = \sum_{i=1}^N H_i \quad (93)$$

with

$$H_i = J_i^{(4)^2} \frac{32}{3} + J_i^{(4)^2} \frac{44}{3} + J_i^{(4)^2} \frac{50}{3} : \quad (94)$$

These VBS states break translational symmetry only up to translations by three lattice spacings. The spinons of this model are again confined through a linear potential, as illustrated below.

energy cost / distance (95)

The conclusions we have drawn for this VBS model rest on the assumption that the quadratic Casimirs of the representations contained in the tensor product shown in the dashed box in (92) as well as in the tensor product one obtains if one shifts this box by one lattice spacing to the left or to the right are smaller than the largest Casimir contained in the tensor product shown in the dotted box in (95). We have verified the validity of this assumption for the $(2,0,0,0)$ VBS model we considered here, but not shown it to hold for similar models with larger n or ℓ .

(4) Finally, consider an $SU(6)$ spin chain with spins transforming under the 70-dimensional representation

$$(1;1;0;0;0) = \begin{array}{|c|c|} \hline \square & \square \\ \hline \end{array} :$$

Thus we have once again $\frac{\Delta}{q} = 2$. In a notation similar to the one introduced for the 8 VBS,

$$\square \triangleq c; \quad \begin{array}{|c|} \hline \square \\ \hline \end{array} \triangleq e;$$

the two degenerate VBSs are illustrated by

projection onto rep. $(1;1;0;0;0)$ (96)

are exact ground states of a parent Hamiltonian involving the quadratic Casimir of the total spin of three neighboring sites,

$$H_{(1;1;0;0;0) \text{ VBS}} = \sum_{i=1}^N H_i \quad (97)$$

with

$$H_i = J_i^{(3)^2} 20 + J_i^{(3)^2} 70 + J_i^{(3)^2} 540 : \quad (98)$$

The states (96) are not the only VBSs one can form. Other possibilities like

or

however, contain additional representations for the total $SU(6)$ spin of three neighboring sites, and are hence expected to possess higher energies.

Spinon excitations transforming under the 6-dimensional rep. $(0;0;0;0;1)$ are linearly confined to spinons transforming under the 15-dimensional rep. $(0;0;0;1;0)$:

energy cost / distance (99)

The VBS configuration we have drawn between the two spinons in (99) constitutes just one of several possibilities. We expect, however, that this possibility corresponds to the lowest energy among them for the Hamiltonian (97). This concludes our list of examples.

The models introduced in this subsection are interesting in that they provide us with examples where spinon confinement, and with the confinement the existence of a Haldane gap, is caused by interactions extending beyond nearest neighbors. The conclusion drawn from the Alicki-Lieb theorem for $SU(n)$ models with spins transforming under representations we have labeled here as the "third category" hence appear to hold for models with nearest-neighbor interactions only, to which the theorem is applicable. For these models, the theorem states that the spectrum is gapless, which according to our understanding implies that the models support deconfined spinon excitations. The examples we have studied, by contrast, suggest that models with longer-ranged interactions belonging to this category exhibit confinement forces between the spinon excitations and hence possess a Haldane gap.

It is worth noting that even though in the examples we elaborated here $\ell < n$, we expect our conclusions to hold for models with $\ell > n$ as well. To see this, let $m > 0$ be an integer such that $nm < \ell < n(m+1)$. We can now construct a first VBS with spinon confinement using nm boxes of the Young tableau and combine it with a second by projection on each side with a second VBS constructed from the remaining $\ell - nm$ boxes. Since the spinons of the first VBS are always confined and hence gapped, the final VBS will support deconfined spinons if and only if the second VBS will support them, which in turn will depend on the largest common divisor q^0 of $\ell - nm$ and n as well as the range of the interaction.

The $SU(4)$ rep. 6 XVBS provides us with an example where a nearest-neighbor Hamiltonian is sufficient to induce spinon condensation and a Haldane gap, even though the largest common divisor of $n = 4$ and $q = 2$ is $q = 2$, i.e., interactions including $\frac{n}{q} = 2$ neighbors would be required following the rules derived from the examples in Sec. XC. The reason for this discrepancy is that in the XVBS model considered here, each site effectively takes the role of two neighboring sites. Aleck et al. [75, 76] conjecture that the ground state of the $SU(4)$ rep. 6 nearest-neighbor Heisenberg model is, like the XVBS reviewed here, two-fold degenerate, which implies that the Aleck-Lieb theorem is not applicable.

This example is valuable in showing that it is advisable to explicitly construct the VBS for a given representation of $SU(n)$ in order to verify the applicability of the general rules motivated above.

XI. CONCLUSION

In the first part of this article, we have formulated several exact models of $SU(3)$ spin chains. We introduced a trimer model and presented evidence that the elementary excitations of the model transform under the $SU(3)$ representations conjugate to the representation of the original spin on the chain. We then introduced three $SU(3)$ valence bond solid chains with spins transforming under representations 6, 10, and 8, respectively. We argued that of these four models, the coloron excitations are condensed only in the 10 and the 8 VBS models, and that only those models with condensed spinons exhibit a Haldane gap. We subsequently generalized three of our models to $SU(n)$, and investigated again which models exhibit spinon condensation.

Finally, we used the rules emerging from the numerous examples we studied to argue that models of $SU(n)$ spin chains in general fall into three categories with regard to spinon condensation and the Haldane gap. These are summarized in the previous subsection. The results rely crucially on the assumption that the conclusions we obtained for the VBS models we studied are of general validity. This assumption certainly holds for the corresponding $SU(2)$ models, and appears reasonable on physical grounds. Ultimately, however, it is only an assumption, or at best a hypothesis.

On a broader perspective, we believe that the models we have studied provide further indication that $SU(n)$ spin chains are an equally rich and rewarding subject of study as $SU(2)$ spin chains have been since Bethe.

ACKNOWLEDGMENTS

We would like to thank Peter Zoller and Peter Woelke, but especially Dirk Schuricht and Ronny Thomale for many highly inspiring discussions of various aspects of this work. We further wish to thank Dirk Schuricht

for valuable suggestions on the manuscript. One of us (SR) was supported by a Ph.D. scholarship of the Bundesministerium.

APPENDIX A: A PROPOSAL FOR AN EXPERIMENTAL REALIZATION OF $SU(3)$ SPIN CHAINS IN AN OPTICAL LATTICE

In this appendix, we wish to describe a proposal for an experimental realization of $SU(3)$ spin chains. The most eligible candidate for such experiments are ultracold gases in optical lattices. Recently, these systems have become an interesting playground for the realization of various problems of condensed matter physics, such as the phase transition from a superfluid to a Mott insulator [77, 78], the fermionic Hubbard model [79, 81], and $SU(2)$ spin chains [82, 83]. In particular, the Hamiltonians for spin lattice models may be engineered with polar molecules stored in optical lattices, where the spin is represented by a single-valence electron of a heteronuclear molecule [84, 85].

In a most naive approach, one might expect to realize an $SU(3)$ spin (at a site in an optical lattice) by using atoms with three internal states, like an atom with spin $S = 1$. If we now were to interpret the $S^z = +1$ state as $SU(3)$ spin "blue", the $S^z = 0$ state as "red", and the $S^z = -1$ state as "green", however, the $SU(3)$ spin would not be conserved. The $SU(2)$ algebra would allow for the process $j \downarrow 1; i \uparrow 0$, which in $SU(3)$ language corresponds to the forbidden process $j \downarrow; i \uparrow$.

A more sophisticated approach is hence required. One way to obtain a system with three internal states in which the number of particles in each state (i.e., of each color) is conserved is to manipulate an atomic system with total angular momentum $F = 3/2$ (where $F = S_{\text{el}} + L_{\text{orb}} + S_{\text{nuc}}$ includes the internal spin of the electrons, the orbital angular momentum, and the spin of the nucleus) to simulate an $SU(3)$ spin. The important feature here is that the atoms have four internal states, corresponding to $F^z = \frac{3}{2}; \frac{1}{2}; +\frac{1}{2}; +\frac{3}{2}$. For such atoms, one has to suppress the occupation of one of the "middle" states, say the $F^z = \frac{1}{2}$ state, by effectively lifting it to a higher energy while keeping the other states approximately degenerate. This can be accomplished through a combination of an external magnetic field and two carefully tuned lasers, which effectively push down the energies of the $F^z = \frac{3}{2}$ and the $F^z = +\frac{1}{2}$ states by coupling these states to states of (say) the energetically higher $F = 5/2$ multiplet (see Fig. 15). At sufficiently low temperatures, we are hence left with a system with three internal states $F^z = \frac{3}{2}; +\frac{1}{2}; +\frac{3}{2}$, which we may identify with the colors "blue", "red", and "green" of an $SU(3)$ spin. In leading order, the number of particles of each color is now conserved, as required by $SU(3)$ symmetry. For example, conservation of F^z forbids processes in which a "blue" and a "green" particle turn into two "red" ones, $j \downarrow; i \uparrow$. Higher order processes of the

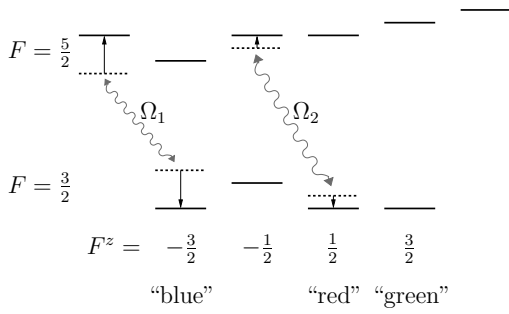


FIG. 15: Effective lifting of the $F^z = -\frac{1}{2}$ state.

kind $\{j;g;g_i\}$ $\{j;r;r_i\}$ are still possible, but negligible if the experiment is conducted at sufficiently short time scales.

If one places fermionic atoms with an artificial SU(3) spin engineered along the lines of this or a related proposal in an optical lattice and allows for a weak hopping of the atoms on the lattice, one has developed an experimental realization of an SU(3) Hubbard model. If the energy cost U of having two atoms on the same lattice site is significantly larger than the hopping t , and the density is one atom per site, the system will effectively constitute an SU(3) antiferromagnet. The dimension of this antiferromagnet will depend on the optical lattice, which can be one-, two-, or three-dimensional.

In principle, the above proposal can be generalized to SU(n), even though the experimental obstacles are likely to grow "exponentially" with n . Besides, it is far from clear that such an endeavor is worthwhile, as all the non-trivial properties of SU(n) are already present in SU(3) chains (while SU(2) constitutes a special case).

APPENDIX B: GELL-MANN MATRICES

The Gell-Mann matrices are given by [67, 68]

$$\begin{aligned}
 1 = \frac{B}{2} \begin{pmatrix} 0 & 1 & 0 \\ 1 & 0 & 0 \\ 0 & 0 & 0 \end{pmatrix} A; \quad 2 = \frac{B}{2} \begin{pmatrix} 0 & i & 0 \\ i & 0 & 0 \\ 0 & 0 & 0 \end{pmatrix} A; \quad 3 = \frac{B}{2} \begin{pmatrix} 1 & 0 & 0 \\ 0 & 1 & 0 \\ 0 & 0 & 0 \end{pmatrix} A; \\
 4 = \frac{B}{2} \begin{pmatrix} 0 & 0 & 1 \\ 0 & 0 & 0 \\ 1 & 0 & 0 \end{pmatrix} A; \quad 5 = \frac{B}{2} \begin{pmatrix} 0 & 0 & i \\ 0 & 0 & 0 \\ i & 0 & 0 \end{pmatrix} A; \quad 6 = \frac{B}{2} \begin{pmatrix} 0 & 0 & 0 \\ 0 & 0 & 1 \\ 0 & 1 & 0 \end{pmatrix} A; \\
 7 = \frac{B}{2} \begin{pmatrix} 0 & 0 & 0 \\ 0 & 0 & i \\ 0 & i & 0 \end{pmatrix} A; \quad 8 = \frac{1}{3} \frac{B}{2} \begin{pmatrix} 1 & 0 & 0 \\ 0 & 1 & 0 \\ 0 & 0 & 2 \end{pmatrix} A;
 \end{aligned}$$

They are normalized as $\text{tr } a^a b^b = 2 \delta_{ab}$ and satisfy the commutation relations $[a^a, b^b] = 2 f^{abc} c^c$. The structure constants f^{abc} are totally antisymmetric and obey Jacobi's identity

$$f^{abc} f^{cde} + f^{bcd} f^{cae} + f^{dac} f^{cbe} = 0;$$

Explicitly, the non-vanishing structure constants are given by $f^{123} = i$, $f^{147} = f^{246} = f^{257} = f^{345} = f^{156} = f^{367} = i/2$, $f^{458} = f^{678} = i/3$, and 45 others obtained by permutations of the indices.

APPENDIX C: EIGENVALUES OF THE QUADRATIC CASIMIR OPERATOR

The eigenvalues of the quadratic Casimir operator for representations $C_{\text{SU}(n)}^2(1; 2; \dots; n-1)$ of SU(n) up to $n = 6$ are given by:

$$C_{\text{SU}(2)}^2(1) = \frac{1}{4} \cdot 2 + 2 = \frac{9}{2} + 1$$

$$C_{\text{SU}(3)}^2(1; 2) = \frac{1}{3} \cdot 2 + 1 \cdot 2 + \frac{2}{2} + 3 \cdot 1 + 3 \cdot 2$$

$$\begin{aligned}
 C_{\text{SU}(4)}^2(1; 2; 3) &= \frac{1}{8} \cdot 3 \cdot 2 + 4 \cdot 2 + 3 \cdot 2 + 4 \cdot 1 \cdot 2 \\
 &+ 2 \cdot 1 \cdot 3 + 4 \cdot 2 \cdot 3 + 12 \cdot 1 + 16 \cdot 2 + 12 \cdot 3
 \end{aligned}$$

$$\begin{aligned}
 C_{\text{SU}(5)}^2(1; 2; 3; 4) &= \frac{1}{5} \cdot 2 \cdot 2 + 3 \cdot 2 + 3 \cdot 2 + 2 \cdot 2 \\
 &+ 3 \cdot 1 \cdot 2 + 4 \cdot 2 \cdot 3 + 3 \cdot 3 \cdot 4 + 2 \cdot 1 \cdot 3 + 1 \cdot 4 \\
 &+ 2 \cdot 2 \cdot 4 + 10 \cdot 1 + 15 \cdot 2 + 15 \cdot 3 + 10 \cdot 4
 \end{aligned}$$

$$\begin{aligned}
 C_{\text{SU}(6)}^2(1; 2; 3; 4; 5) &= \\
 &\frac{1}{12} \cdot 5 \cdot 2 + 8 \cdot 2 + 9 \cdot 2 + 8 \cdot 2 + 5 \cdot 2 \\
 &+ 8 \cdot 1 \cdot 2 + 12 \cdot 2 \cdot 3 + 12 \cdot 3 \cdot 4 + 8 \cdot 4 \cdot 5 \\
 &+ 4 \cdot 1 \cdot 4 + 6 \cdot 1 \cdot 3 + 8 \cdot 2 \cdot 4 + 6 \cdot 3 \cdot 5 \\
 &+ 4 \cdot 2 \cdot 5 + 2 \cdot 1 \cdot 5 + 30 \cdot 1 + 48 \cdot 2 \\
 &+ 54 \cdot 3 + 48 \cdot 4 + 30 \cdot 5
 \end{aligned}$$

The general method to obtain these and further eigenvalues for $n > 6$ requires a discussion of representation theory [74] at a level which is beyond the scope of this article.

The dimensionality of a representation $(1; 2; \dots; n-1)$ is determined by the so-called Hook formula [67]

$$\dim = \frac{\prod_{i < j} (i_j + j_i)}{\prod_{i < j} (j_i - i_i)}; \quad (C1)$$

where $i_i = \prod_{j=i}^{n-1} j$ for $i = 1; \dots; n$. In particular, it yields for $n = 2; 3; 4$:

$$\dim_{\text{SU}(2)}(1) = 2 + 1$$

$$\dim_{\text{SU}(3)}(1; 2) = \frac{1}{2} (1+1)(2+1)(1+2+2)$$

$$\begin{aligned}
 \dim_{\text{SU}(4)}(1; 2; 3) &= \frac{1}{12} (1+1)(2+1)(3+1) \\
 &(1+2+2)(2+3+2)(1+2+3+3)
 \end{aligned}$$

-
- [1] H. Bethe, *Z. Phys.* 71, 205 (1931), translated in D. C. Mattis, ed., *The Many-Body Problem* (World Scientific, Singapore, 1993).
- [2] C. N. Yang, *Phys. Rev. Lett.* 19, 1312 (1967).
- [3] R. J. Baxter, *Exactly Solved Models in Statistical Mechanics* (Academic Press, London, 1990).
- [4] V. E. Korepin, N. M. Bogoliubov, and A. G. Izergin, *Quantum Inverse Scattering Method and Correlation Functions* (Cambridge University Press, Cambridge, 1997).
- [5] L. D. Faddeev and L. A. Takhtajan, *Phys. Lett. A* 85, 375 (1981).
- [6] R. B. Laughlin, *Phys. Rev. Lett.* 50, 1395 (1983).
- [7] *Quantum Hall Effect*, edited by M. Stone (World Scientific, Singapore, 1992).
- [8] F. D. M. Haldane, *Phys. Lett. A* 93, 464 (1983).
- [9] F. D. M. Haldane, *Phys. Rev. Lett.* 50, 1153 (1983).
- [10] I. A. A. Eck, in *Fields, strings and critical phenomena*, Vol. XLIX of *Les Houches lectures*, edited by E. Brezin and J. Zinn-Justin (Elsevier, Amsterdam, 1990).
- [11] E. Fradkin, *Field Theories of Condensed Matter Systems*, No. 82 in *Frontiers in Physics* (Westview Press, Boulder, 1991).
- [12] A. O. Gogolin, A. A. Nersisyan, and A. M. Tsvelik, *Bosonization and Strongly Correlated Systems* (Cambridge University Press, Cambridge, 1998).
- [13] T. Giamarchi, *Quantum Physics in One Dimension* (Oxford University Press, Oxford, 2004).
- [14] C. K. Majumdar and D. K. Ghosh, *J. Math. Phys.* 10, 1399 (1969).
- [15] I. A. A. Eck, T. Kennedy, E. H. Lieb, and H. Tasaki, *Phys. Rev. Lett.* 59, 799 (1987).
- [16] I. A. A. Eck, T. Kennedy, E. H. Lieb, and H. Tasaki, *Commun. Math. Phys.* 115, 477 (1988).
- [17] F. D. M. Haldane, *Phys. Rev. Lett.* 60, 635 (1988).
- [18] B. S. Shastry, *Phys. Rev. Lett.* 60, 639 (1988).
- [19] F. D. M. Haldane, *Phys. Rev. Lett.* 66, 1529 (1991).
- [20] F. D. M. Haldane, Z. N. C. Ha, J. C. Talstra, D. Bernard, and V. Pasquier, *Phys. Rev. Lett.* 69, 2021 (1992).
- [21] F. D. M. Haldane, *Phys. Rev. Lett.* 67, 937 (1991).
- [22] Z. N. C. Ha and F. D. M. Haldane, *Phys. Rev. B* 47, 12459 (1993).
- [23] F. H. L. E. ler, *Phys. Rev. B* 51, 13357 (1995).
- [24] M. G. reiter and D. Schuricht, *Phys. Rev. B* 71, 224424 (2005).
- [25] M. G. reiter, *Statistical Phases and Momentum Spacings for One-Dimensional Anyons*, submitted to *Phys. Rev. Lett.*
- [26] M. G. reiter and D. Schuricht, *Many-spinon states and the secret significance of Young tableaux*, submitted to *Phys. Rev. Lett.*
- [27] N. Kawakami, *Phys. Rev. B* 46, 1005 (1992).
- [28] N. Kawakami, *Phys. Rev. B* 46, R3191 (1992).
- [29] Z. N. C. Ha and F. D. M. Haldane, *Phys. Rev. B* 46, 9359 (1992).
- [30] P. Bouwknegt and K. Schoutens, *Nucl. Phys. B* 482, 345 (1996).
- [31] D. Schuricht and M. G. reiter, *Europhys. Lett.* 71, 987 (2005).
- [32] D. Schuricht and M. G. reiter, *Phys. Rev. B* 73, 235105 (2006).
- [33] R. Jullien and F. D. M. Haldane, *Bull. Am. Phys. Soc.* 28, 344 (1983).
- [34] I. A. A. Eck, *J. Phys.: Condens. Matter* 1, 3047 (1989).
- [35] K. Okamoto and K. Nomura, *Phys. Lett. A* 169, 433 (1992).
- [36] S. Eggert, *Phys. Rev. B* 54, R9612 (1996).
- [37] S. R. White and I. A. A. Eck, *Phys. Rev. B* 54, 9862 (1996).
- [38] D. Sen and N. Surendran, *Phys. Rev. B* 75, 104411 (2007).
- [39] S. Knabe, *J. Stat. Phys.* 52, 627 (1988).
- [40] M. Fannes, B. Nachtergaele, and R. F. Werner, *Europhys. Lett.* 10, 633 (1989).
- [41] W. D. Freitag and E. M. Ullrich-Hartmann, *Z. Phys. B* 83, 381 (1991).
- [42] A. Klumper, A. Schadschneider, and J. Zittartz, *J. Phys. A* 24, L955 (1991).
- [43] T. Kennedy and H. Tasaki, *Phys. Rev. B* 45, 304 (1992).
- [44] A. Klumper, A. Schadschneider, and J. Zittartz, *Z. Phys. B* 87, 281 (1992).
- [45] A. Klumper, A. Schadschneider, and J. Zittartz, *Europhys. Lett.* 24, 293 (1993).
- [46] M. T. Batchelor and C. M. Yung, *Int. J. Mod. Phys. B* 8, 3645 (1994).
- [47] U. Schollwöck, T. Jolicoeur, and T. Garel, *Phys. Rev. B* 53, 3304 (1996).
- [48] A. Kolezhuk, R. Roth, and U. Schollwöck, *Phys. Rev. Lett.* 77, 5142 (1996).
- [49] A. Kolezhuk and U. Schollwöck, *Phys. Rev. B* 65, 100401(R) (2002).
- [50] B. Normand and F. Mila, *Phys. Rev. B* 65, 104411 (2002).
- [51] A. Lauchli, G. Schmid, and S. Trebst, *Phys. Rev. B* 74, 144426 (2006).
- [52] B. Sutherland, *Phys. Rev. B* 12, 3795 (1975).
- [53] T. C. Choy and F. D. M. Haldane, *Phys. Lett. A* 90, 83 (1982).
- [54] Y. Q. Li, M. Ma, D. N. Shi, and F. C. Zhang, *Phys. Rev. B* 60, 12781 (1999).
- [55] S. J. Gu and Y. Q. Li, *Phys. Rev. B* 66, 092404 (2002).
- [56] J. Dammerau and A. Klumper, *J. Stat. Mech.* 12014 (2006).
- [57] N. Kawashima and Y. Tanabe, *Phys. Rev. Lett.* 98, 057202 (2007).
- [58] A. Paramakanti and J. B. Marston, cond-mat/0608691.
- [59] I. A. A. Eck, *Nucl. Phys. B* 265, 409 (1986).
- [60] I. A. A. Eck, *Nucl. Phys. B* 305, 582 (1988).
- [61] S. Chen, C. Wu, S. C. Zhang, and Y. Wang, *Phys. Rev. B* 72, 214428 (2005).
- [62] S. Chen, Y. Wang, W. Q. Ning, C. Wu, and H. Q. Lin, *Phys. Rev. B* 74, 174424 (2006).
- [63] I. A. A. Eck and E. H. Lieb, *Lett. Math. Phys.* 12, 57 (1986).
- [64] M. G. reiter, S. Rachel, and D. Schuricht, *Phys. Rev. B* 75, 060401(R) (2007).
- [65] P. M. van den Broek, *Phys. Lett. A* 77, 261 (1980).
- [66] T. Inui, Y. Tanabe, and Y. Onodera, *Group Theory and Its Applications in Physics* (Springer, Berlin, 1996).
- [67] J. F. Cornwell, *Group theory in physics* (Academic Press, London, 1984), Vol. II.
- [68] H. Georgi, *Lie Algebras in Particle Physics* (Addison-Wesley, Redwood City, 1982).
- [69] J. Schwinger, in *Quantum Theory of Angular Momentum*

- tum, edited by L. Biedenharn and H. van Dam (Academic Press, New York, 1965).
- [70] A. Auerbach, *Interacting electrons and quantum magnetism* (Springer, New York, 1994).
 - [71] M. Greiter, *Phys. Rev. B* **65**, 134443 (2002).
 - [72] M. Greiter, *Phys. Rev. B* **66**, 054505 (2002).
 - [73] A. J. Macfarlane, A. Sudbery, and P. H. Weiss, *Commun. Math. Phys.* **11**, 77 (1968).
 - [74] J. E. Humphreys, *Introduction to Lie Algebras and Representation Theory* (Springer, New York, 1987).
 - [75] I. A. A. de Sá, D. P. A. rovas, J. B. M. arston, and D. A. R. abson, *Nucl. Phys. B* **366**, 467 (1991).
 - [76] J. B. M. arston and I. A. eck, *Phys. Rev. B* **39**, 11538 (1989).
 - [77] D. Jaksch, C. Bruder, J. I. Cirac, C. W. Gardiner, and P. Zoller, *Phys. Rev. Lett.* **81**, 3108 (1998).
 - [78] M. Greiner, O. Mandel, T. Esslinger, T. W. Hansch, and I. Bloch, *Nature* **415**, 39 (2002).
 - [79] C. Honerkamp and W. Hofstetter, *Phys. Rev. Lett.* **92**, 170403 (2004).
 - [80] C. Honerkamp and W. Hofstetter, *Phys. Rev. B* **70**, 094521 (2004).
 - [81] A. Rapp, G. Zarand, C. Honerkamp, and W. Hofstetter, *cond-mat/0607138*.
 - [82] L. M. Duan, E. Demler, and M. D. Lukin, *Phys. Rev. Lett.* **91**, 090402 (2003).
 - [83] J. J. Garcia-Ripoll, M. A. Martin-Delgado, and J. I. Cirac, *Phys. Rev. Lett.* **93**, 250405 (2004).
 - [84] A. Micheli, G. K. Brennen, and P. Zoller, *Nature Phys.* **2**, 341 (2006).
 - [85] G. K. Brennen, A. Micheli, and P. Zoller, *quant-ph/0612180*.

